2013

Process optimization: Ultrasonic welding of coextruded polymer film

Jessica Ann Riedl
Iowa State University

Process optimization: Ultrasonic welding of coextruded polymer film

by

Jessica Ann Riedl

A thesis submitted to the graduate faculty

in partial fulfillment of the requirements for the degree of

MASTER OF SCIENCE

Major: Agricultural Engineering

Program of Study Committee:
David A. Grewell, Major Professor
Michael Kessler
D. R. Raman

Iowa State University

Ames, Iowa

2013

TABLE OF CONTENTS

LIST OF TABLES

LIST OF FIGURES

ABSTRACT

The purpose of this research is to determine the effect of various weld and machine parameters on ultrasonic weld strength. Specifically, welds with six different triple-layer coextruded polyethylene and metallized polypropylene films were examined. These materials were welded in separate experimental studies using a bench top weld system and a high production volume packaging machine.

The first study investigated the effect of a range of weld forces, energies, and amplitudes in a lap joint geometry using a bench top ultrasonic plunge welding system. Weld strength was determined by measuring resistance to tearing and peel and shear strength. It was observed that low energy and low weld force had a significant effect on shear strength welds for all materials. High peel strength was observed at relatively high weld forces and energies, and high tear resistance was observed at relatively high forces, high amplitudes, and mid-range energy levels.

The second study determined the suitability for the same materials to be sealed as bags for packaging applications in a vertical “form fill seal” machine. This machine was equipped with an ultrasonic end seal jaw. The machine factors tested in this study include energy, amplitude, and production rate (the rate at which bags are created/welded) to determine the effect on peel strength. It was observed that low energy and amplitude correlated with high strength for the top weld (top of bag) of one material and low production rate resulted in high strength for the top weld of two materials as well as the bottom weld for two materials. Data for the sixth material was inconclusive.

CHAPTER 1. GENERAL INTRODUCTION

The purpose of this research was to characterize the weld strength of six different, triple-layer coextruded polyethylene and metallized polypropylene films. These materials were welded on both a bench top ultrasonic plunge welding system and a vertical form fill seal (FFS) machine with ultrasonic end seals. Weld configuration (bench top and FFS machine) and machine parameters were varied to determine their effects on weld peel strength, shear strength, and tearing force. The purpose of this chapter is to provide background information regarding packaging applications for polymers and basic ultrasonic welding theory, as well as to describe the six materials that are examined in Chapters 2 and 3.

Plastic Packaging

The global packaging market, valued at $429 billion and employing over five million people in 2009 [1], is steadily growing. As the market expands and increases the scarcity of resources, it will be advantageous for producers to minimize non-renewable resources consumed by packaging. These resources include, but are not limited to, process and product inputs such as raw materials, water, and energy as well as process outputs such as waste chemicals, pollutants, and scrap materials. Groups such as the International Standards Organization [1] and Sustainable Packaging Coalition (SPC) support efforts to create guidelines to identify packaging materials and practices that are most sustainable, considering global economic and environmental health [2].

Plastic packaging is expected to be the fastest-growing segment of sustainable packaging [1]. Plastic products, including packaging, often attract criticism because most are based on nonrenewable petroleum, typically not recycled at end-of-life, and usually non-compostable. However, there are also many reasons why plastics are used for packaging: these products are moldable, generally chemical inert, cost effective, lightweight, and versatile in transparency, color, heat resistance, vapor barrier, and heat sealable [3].

Traditionally polymer film bags were created using heat seals or adhesives. However, heat sealing is a relatively lengthy and energy inefficient process because of thermal radiation losses when the heated tools are idle. Use of adhesives may create hazardous waste and require protective equipment for personnel.

Ultrasonic Welding

Thermoplastics were first joined by ultrasonic energy in the late 1960s. Benefits of ultrasonic welding include high speed, efficiency, lack of material contamination, and no required consumables. Ultrasonic welding systems perform with high consistency, provide uniform joint quality and are very fast with weld times typically less than a second [4]. Because of these benefits, the use of ultrasonic energy has become an increasingly common method to join plastics for applications such as packaging, electronic components, automotive, and consumer products, despite high initial cost and limitations regarding part size and design [5].

Use of ultrasonics for plastic joining inherently meets two criteria developed by SPC for sustainable packaging, 1) “physically designed to optimize materials and

energy" and 2) "manufactured using clean production technologies and best practices" [2]. Ultrasonic welding achieves both of these goals because it does not require the use of any mechanical fasteners or chemical adhesives and it utilizes energy for the minimum time required to create a weld [6].

Figure 1 Branson 200X 30 kHz digitally controlled actuator

Ultrasonic weld systems consist of four main components, including a power supply, and the transducer, booster, and horn, a combination known as the stack and actuator. An anvil supports the work pieces below the stack. A solid-state power supply converts 50 or 60 Hz standard current to a 10 to 70 kHz signal, which the

transducer then converts to mechanical vibrations, typically by way of piezoelectric materials. The booster, and often the horn, amplify the vibration, typically between 1 and 250 μm, and apply it to the parts. This vibration causes cyclical deformation in the surface asperities of the parts at the joining surface [5].

Because polymers are viscoelastic, some of the mechanical energy applied to the surface asperities is recovered, but the remainder is dissipated as thermal energy (heat). This behavior is represented by a complex dynamic modulus, E^*, which has a real part, storage modulus, E', and an imaginary part, loss modulus, E'', shown in Equation (1). Enough heat is released because of this cyclical deformation to melt and fusion-bond the material at the joining surfaces [6].

$$E^* = E' + iE'' \tag{1}$$

The rate of heat loss, $\dot{Q}$, (W/m^3), in the material can be described as a function of the loss modulus of the material and the angular frequency, ω, and strain of the deformation, ε_0, which is generally directly proportional to the vibration amplitude. Even though the loss modulus is difficult to measure and is unknown for the materials used in these studies, it is clear from Equation (2) that increasing the vibration amplitude (proportional to strain) will result in faster heating [6].

$$\dot{Q} = \frac{E''\omega\varepsilon_0^2}{2} \tag{2}$$

At the same time that ultrasonic energy is activated, the horn is also applying a normal force to the welding surfaces. When the asperities reach the melt temperature, they begin to flow and the increased weld force will also increase this

flow under pressure, known as squeeze flow. Squeeze flow orients the long polymer chains parallel to the direction of flow, which reduces weld strength in at least two ways. First, it makes them more susceptible to cracking, and second, it results in fewer secondary bonds between the two materials and less molecular entanglement [6].

Squeeze flow also allows filling of the voids between asperity peaks and at limited flow rates it can promote entanglement of the molecules thus enhancing bond strength. After the interfaces have completely conformed to each other, the polymer chains diffuse across the weld interface and become entangled. This is known as interfacial healing. Once healing is complete and ultrasonic energy has been deactivated, the interface cools and solidifies [5].

In Chapter 2, weld force, energy, and amplitude were varied to identify a range of operating parameters for a bench top system that results in optimal weld strength as determined by peel strength, shear strength, and tearing force. In Chapter 3 the experimental design varied the ultrasonic energy and amplitude and the production rate of a high speed packaging machine to again determine parameters resulting in optimal weld strength as determined by peel strength.

Experimental Materials

Commonly seen in packaging applications is the combination of up to seven layers of different plastic films. A process known as coextrusion combines layers of film in order to capitalize on a combination of properties that the individual components alone cannot achieve [3]. For example, one layer may provide

resistance to ultraviolet light, another provides chemical resistance, and yet another provides puncture resistance. In the two studies detailed in this thesis, six grades of proprietary 200 gage (0.05 mm thick) triple-layer coextruded polyethylene (PE) and polypropylene (PP) film were examined. These materials were not commercially available and had been supplied by an anonymous manufacturer.

Like for all polymers, there are many grades and densities of polyethylene. Information regarding the specific material properties of the polyethylene film used in this study was not provided by the manufacturer. However, linear low density polyethylene is commonly used for film applications because of its good tensile strength as well as puncture, tear, and impact resistance properties. Applications include produce bags, garbage bags, stretch wrap, industrial liners, diaper liners, and shopping bags [7].

Polypropylene differs chemically from PE in that it has a stiffening methyl group attached to every other carbon atom. This results in a higher melting point and tensile strength for PP. Polypropylene film is commonly used for packaging because it has excellent chemical resistance and flexibility [7]. Grewell et al. also rate PP "easiest" for general weldability [6] and according to the American Welding Society, polypropylene can be welded to itself [8].

The anonymous material supplier provided the proprietary films in the form of 450 m × 0.343 m rolls. Each coextruded film consisted of a polyethylene layer sandwiched between a metallized oriented polypropylene (OPP) layer and a variable OPP layer. Metallization of the OPP layer occurs during the extrusion

process when a gaseous metal is blown over the film. All specimens in both studies were completed with the material folded so the inside metallized OPP layers were at the weld interface, or faying surface. The variable layers were adjacent to the horn and anvil as shown in Figure 2.

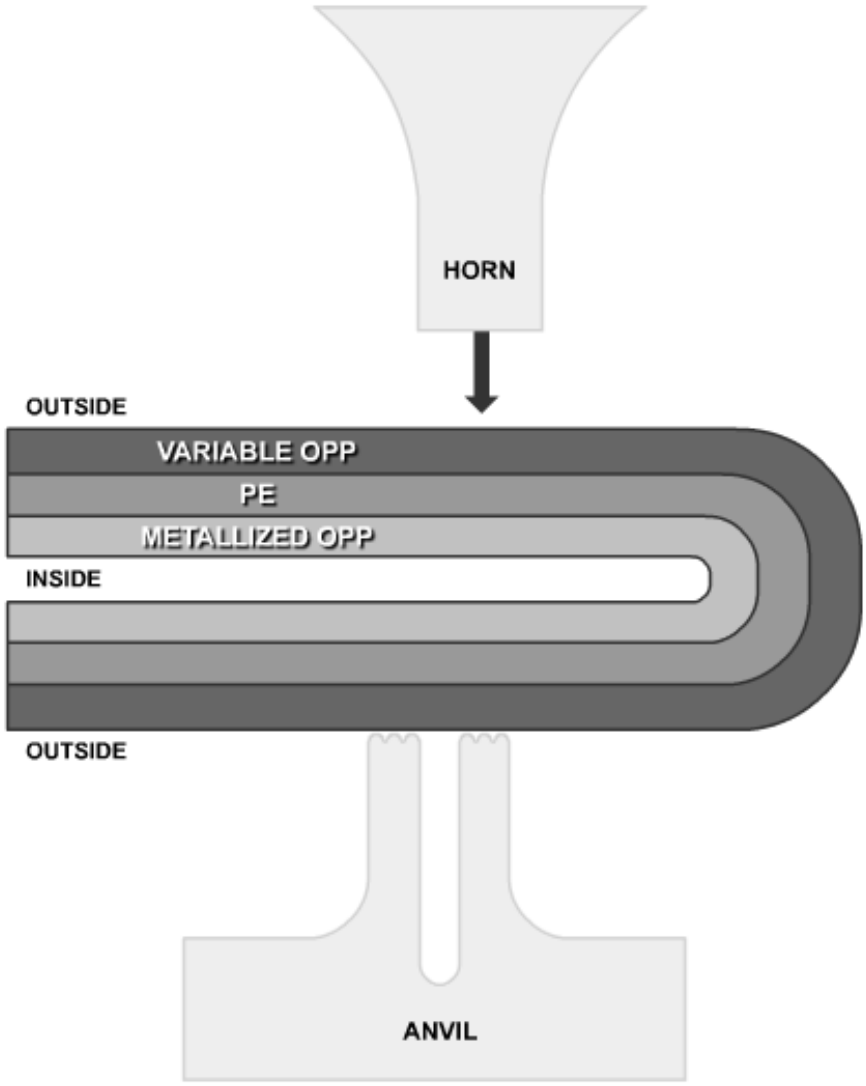

Figure 2 Schematic of film orientation in bench top weld system

The supplier indicated that both OPP layers were heat sealable. The variable layers differed in thickness, stiffness, and coefficient of friction. The variable layers

for the F2A, F2B, and F8 materials were slip modified to lower the coefficient of friction resulting in faster, more efficient processing and package manufacturing. It is unknown whether the film was produced by casting or blowing or whether it was oriented in the machine or transverse direction or both. The differences in the OPP layers are summarized in Table 1.

Table 1 Distinguishing characteristics of variable OPP layers

Material ID	**Distinguishing Characteristics**	**Weight (g)**
F2A	Printable, Lower Coefficient of Friction	70
F2B	Printable, Lower Coefficient of Friction	90
F8	Lower Coefficient of Friction	90
CB	High barrier	80
PW	Metallized	70
YH	Metallizable	70

Thesis Organization

Chapters 2 and 3 are modified journal articles that both explain experimental characterizations of the polyolefin film materials described in this chapter. Chapter 2 investigates the peel strength, shear strength, and tearing force responses of materials welded on a bench top system. Chapter 3 details research that examined the peel strength of the top and bottom seals of bags created in a vertical form, fill, seal packaging machine. Chapter 4 summarizes the conclusions drawn from both studies and offers recommendations for future investigation. References for the contents of each chapter are aggregated prior to the Appendices.

CHAPTER 2. PEEL AND SHEAR STRENGTH AND TEAR RESISTANCE OF ULTRASONICALLY SEALED COEXTRUDED POLYOLEFIN FILMS FOR PACKAGING APPLICATIONS

Modified from a paper to be submitted to *Polymer Engineering and Science*

J. Riedl, D. Grewell, D. R. Raman[1], M. Kessler[2]

Abstract

The aim of this study was to identify the set of welding parameters that yields the highest weld strengths in six different triple-layer, coextruded polyolefin films. The parameters investigated include weld forces, energy delivery, and amplitude. Welds were made using an ultrasonic plunge welding system. Weld performance was determined by peel and shear strength and tearing force.

It was observed that energy and weld force had a significant effect on peel strength for the majority of the materials and the highest peel strength was found at high weld forces and high energies for all materials. Low weld energy and low weld force were observed to produce high shear strength welds for all materials. However, the results for tearing force were inconsistent amongst all six materials.

---

[1] Department of Agricultural and Biosystems Engineering, Iowa State University, Ames, Iowa 50010
[2] Department of Materials Science and Engineering, Iowa State University, Ames, Iowa 50010

The highest tear resistance was found with welds created with the highest force and amplitude and at mid-range energy levels.

Introduction

This study focused on characterizing the strength of ultrasonic welds made in the six polyolefin films. Welds similar to these can be used to seal film of various materials creating bags used for packaging. These seals create a barrier protecting products from air, water, and chemical infiltration. Bags of this type are used for packaging foods, such as potato chips, as well as other applications.

Ultrasonic welding systems are typically controlled by factors such as horn and anvil size and shape, frequency, amount of energy delivered, weld time, joint type, and weld force (the normal force applied to the part [5]). For manufacturing, it is critical to identify a suitable combination of weld parameters in order to meet the design requirements for the product specification (joint performance). One of the most critical requirements is weld strength. Weld strength can be determined in a number of ways and this study, three approaches were examined: peel strength, shear strength, and tearing force.

Several welding parameters were varied during preliminary welding trials at Branson Ultrasonics Corporation (BUC) (Danbury, CT) in order to identify the boundaries of an experimental design space that could be investigated in more detail. These parameters included several discrete energy levels, ranging from 200 to 400 J, three discrete amplitudes from 0.025 to 0.032 mm, and three discrete weld forces, from 412 to 620 N.

Welds created using these initial parameters were inspected visually and findings were documented. Evidence of excessive welding, known as over weld, is shown in Figure 3. An example of a weld not fully sealed for the length of the horn and anvil, also known as under weld, is shown in Figure 4. Welds were also inspected for contamination.

Figure 3 Excessive over weld condition

Figure 4 A complete weld (left) and example of under weld (right)

The final experimental design space and various settings that were studied are detailed in Table 2. Trigger force, the force threshold at which ultrasonic energy

is activated [5], was not varied independently and was set to 95% of weld force. All other processing factors such as frequency and joint type, horn and anvil design, were held constant. There were 45 total process parameter combinations in the full factorial experimental design and five weld specimens of each of the six materials were made during each treatment. All welds were analyzed for three response variables: peel strength, shear strength, and tearing force.

Table 2 Design of experiment factors

Factors	**Levels**
Energy (J)	400
	300
	250
	200
	100
Amplitude (mm)	0.032
	0.029
	0.025
Weld Force (N)	620
	517
	412

It was believed that all three of these variables—weld energy, amplitude, and force—would affect weld strength as these parameters affect heating, squeeze flow, and interfacial healing [6]. The objective of this study was to identify the set of parameters that yields the highest weld strength.

Experimental Procedure

All welds for this study were created at BUC using a 30 kHz Branson 2000X 1500 W power supply, single converter, and gold booster with a gain of 1:1.5. The 3:1 gain horn was a Branson rectangular slotted riser back made of uncoated titanium. It was 152.4 mm long with a 12.7 mm wide front face and a 38.1 mm back stock. The anvil was solid hardened steel with a triple solid bar pattern, which is a common configuration for packaging. The Branson 2000X system was set to the energy mode, meaning that the power supply monitors the dissipated power as a function of time and discontinues the weld cycle once a preselected value of energy has been delivered to the part [6].

Table 3 Typical ultrasonic welding cycle [6]

Step		**Typical Time (s)**
Load parts	Manually	3 – 5
	Automated	0.1 – 3
Press palm buttons to activate process	Manually	1 – 2
	Automated	0 – 0.5
Head lowers		0.25 – 2
Ultrasonic energy on		0.1 – 10
Hold time		0.1 – 10
Head raises		0.25 – 2
Remove parts	Manually	3 – 5
	Automated	0.1 – 3

Specimens were cut to approximately 350 mm × by 200 mm rectangles and folded in half. The folded end was secured in a clamp. The remainder was stretched

over an anvil and secured as shown in Figure 5, and the welder was actuated. The specimen was labeled and the following data was documented: material ID, cycle number, specimen number, energy, amplitude, weld force, and trigger force. Table 3 shows the typical weld operations and cycle times for each operation.

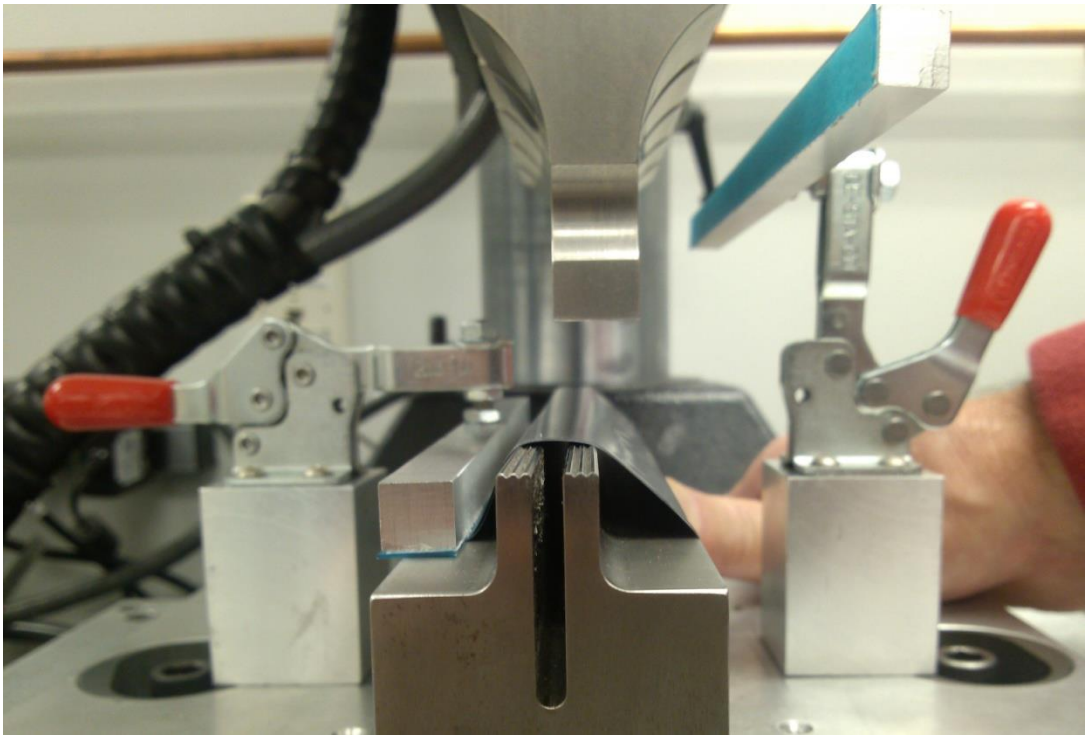

Figure 5 Photograph of weld configuration

The resultant specimens had a cross-section as shown in Figure 6. The welded seal was 152.4 mm wide and approximately 38 mm from the fold. Three samples were cut from each weld specimen and each was subjected to a different physical performance test: tearing force, peel, and shear strength as shown in Figure 7.

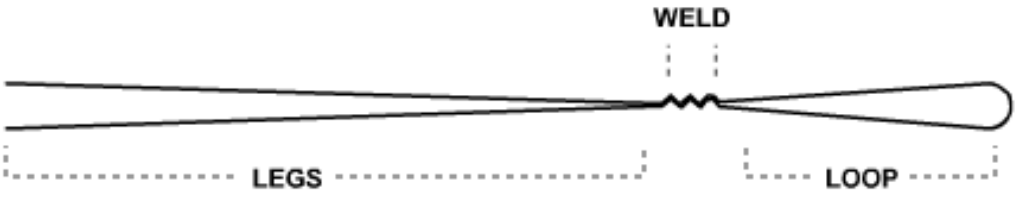

Figure 6 Diagram of cross-section of welded specimen

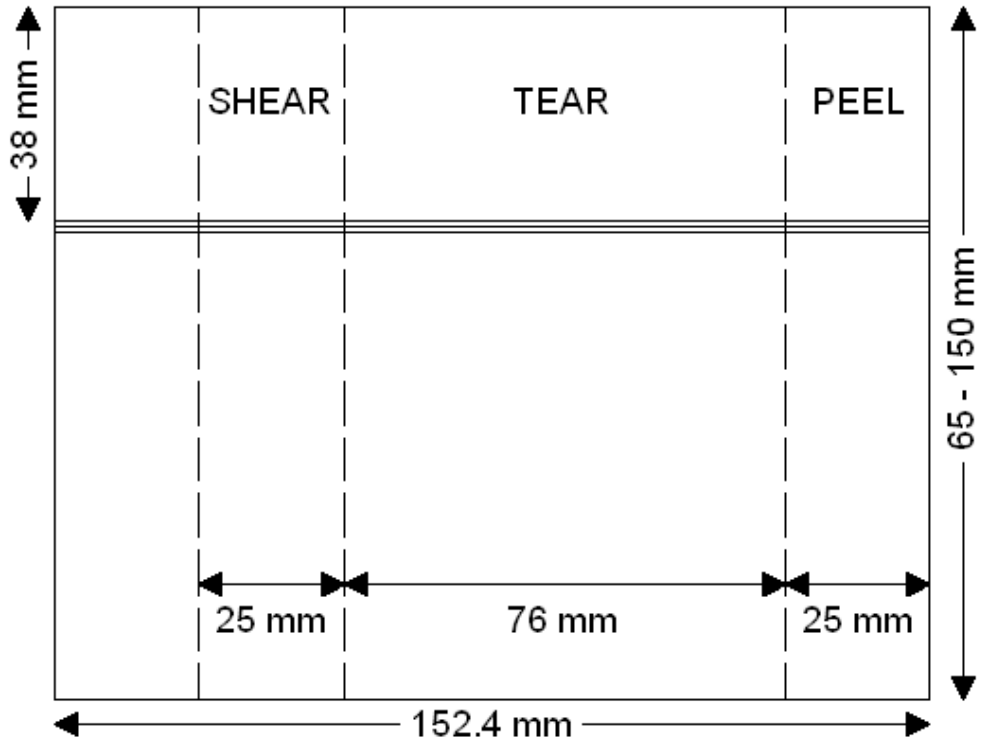

Figure 7 Schematic of individual test specimen locations for weld specimen

Peel Strength Testing

Peel strength was determined by a procedure based on the ASTM International D882-12 Standard Test Method for Tensile Properties of Thin Plastic Sheeting [9] though the elongation aspects of ASTM D882 were not used. Specimens met the size and shape requirements outlined in ASTM D882. Specimens were cut to

25 mm width using a paper cutter with a sliding metal blade. Specimen length varied from 65 to 150 mm, and specimens of excessive length were trimmed using ceramic scissors.

Peel strength measurements were taken using an Instron (Norwood, MA) Model 4502 load frame with grip distance of 50 mm and crosshead speed of 25 mm/min. Mechanical wedge action grips were used, and the grip surface was covered with 0.5 mm thick Nexcare Absolute Waterproof First Aid Tape to prevent slip and puncture of the specimens because of the sharp diamond serrated finish on the face of the jaw grips.

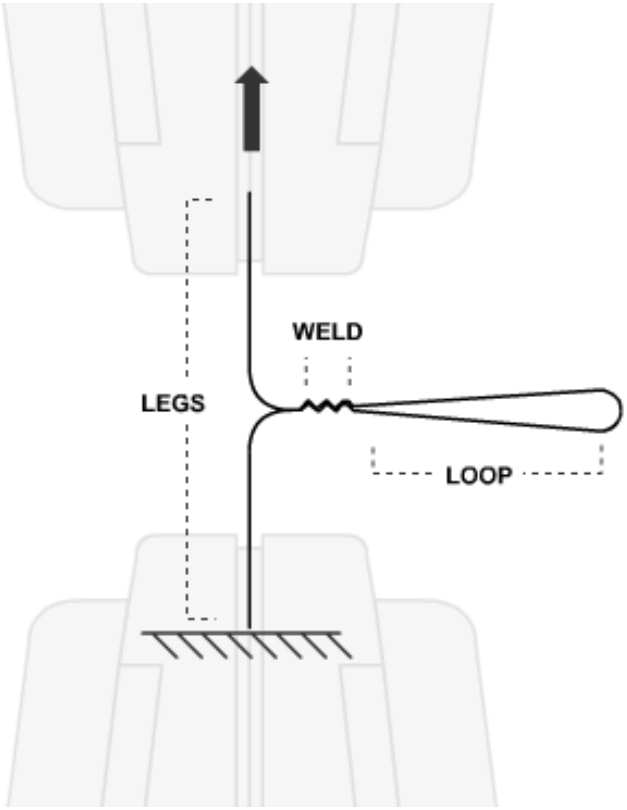

Figure 8 Diagram of specimen placement for peel strength testing

Both legs of the sample were placed into the grips such that the weld was centered between the grips as shown in Figure 8. The bottom grip remained stationary and the top grip traveled 20 mm upward or until the weld failed. The measured maximum load was documented.

Shear Strength Testing

Shear strength was also determined by a procedure based on ASTM D882 [9]. Again, the elongation specifications of the standard were not used. Specimens were cut to the same dimensions using the same method as for peel strength testing described above. However, the loop in the specimens was cut so the cross-section would resemble an "X".

Shear strength measurements were made with the Instron Model 4502 load frame, with grip distance of 50 mm and crosshead speed of 25 mm/min. Mechanical wedge action grips were again covered with 0.5 mm thick Nexcare Absolute Waterproof First Aid Tape to prevent slip and puncture of the specimens.

Figure 9 Photograph of specimen placement for shear strength testing

The top right leg of the "X" was placed in the top jaw grip, and the bottom left leg was secured in the bottom jaw grip as shown in Figure 9. The weld was centered between the grips while maintaining at least 6 mm of film in the grips. The bottom grip remained stationary, and the top grip traveled 75 mm upward or until the weld failed. The measured maximum load was documented and used to calculate the stress endured based on the area of the three bar pattern on the anvil over the width of the test specimen, 3×(0.6 mm × 25 mm). The maximum shear stress sustained prior to failure is equivalent to shear strength [10].

Tear Resistance Testing

Tear force was measured according to ASTM D1922-09 Standard Test Method for Propagation Tear Resistance of Plastic Film and Thin Sheeting by Pendulum Method [11]. This method measures the energy absorbed by the specimen when a tearing force is applied to a pre-existing slit in the material. Specimens were cut using ceramic scissors in compliance with the template as shown in Figure 10.

Measurements were made with an Oakland Instruments Model ME-800 Elmendorf Tear Tester (Minneapolis, MN) outfitted with an 800 g pendulum. Specimens were clamped into the vice with the constant radius section pointing upward. The slit was centered between the twin vise jaws. One jaw was connected to the tester base and kept stationary throughout the test. The other jaw was attached to and thus moved along with the pendulum.

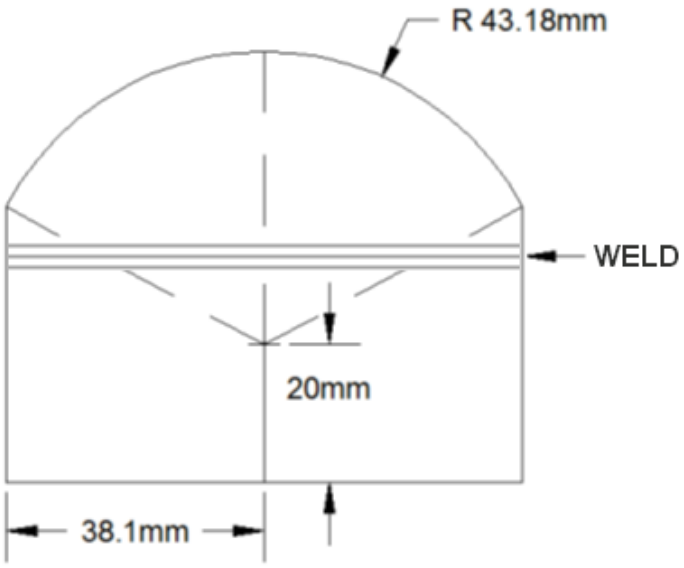

Figure 10 ASTM D 1922 tear propagation template [11]

Prior to testing, the pendulum was swung without a specimen in the vice to verify that the pointer reported a zero reading. The orientation in Figure 11 shows the beginning of the test, when the pendulum was secured at its maximum height and potential energy position. To initiate the test, a release was pressed and the pendulum swung. The pendulum slowed as it tore the film, indicating that some of the kinetic energy from its motion was absorbed by the specimen [12]. After specimen failure, the pendulum was stopped and the test result was read from the indicator on the pendulum.

The result was a percentage of maximum potential energy. This result was used to calculate tearing force (in units of force) as shown in Equation 3. A reading of 100% indicates that all potential energy of the pendulum was absorbed by tearing the specimen. For example, for a tearing force reading of 5% the tearing force would be 392 mN as shown in Equation (3) [11].

$$5 \times 8\ g \times 9.81\ \frac{m}{s^2} = 392\ mN \qquad (3)$$

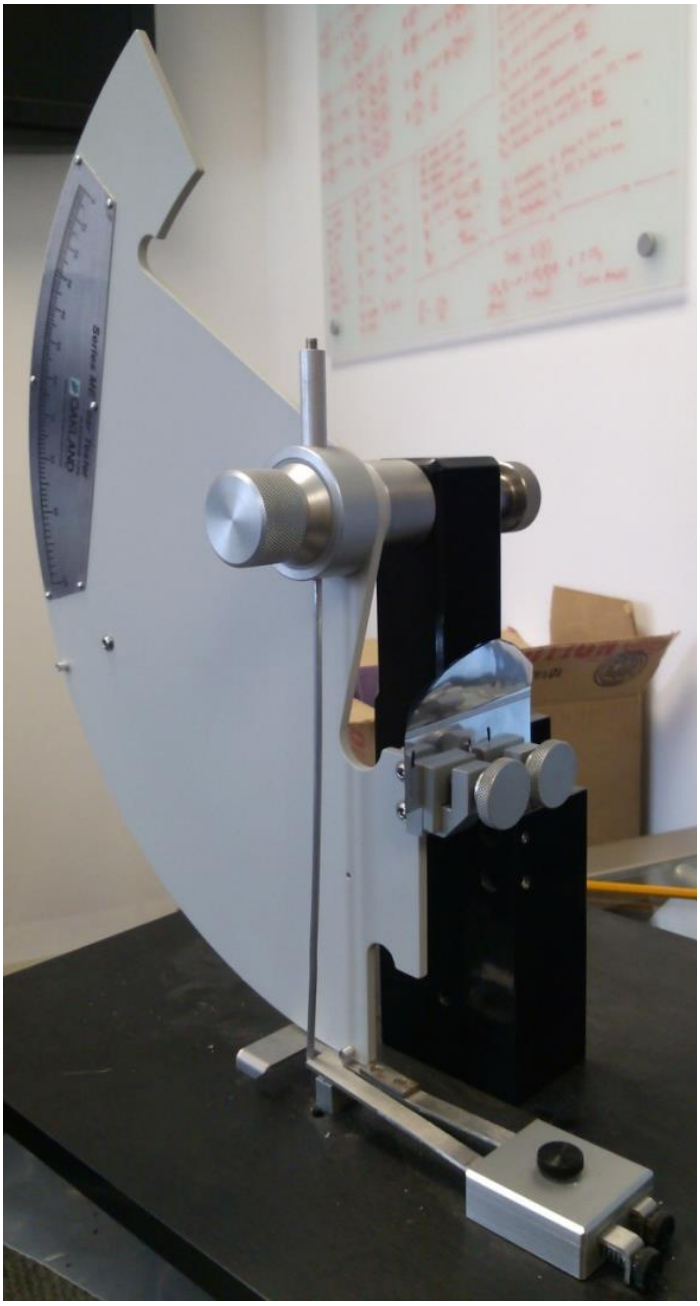

Figure 11 Specimen prior to tearing force testing

Results and Discussion

The three objectives of the experiments described in this chapter were to determine the optimum 1) weld force, 2) amplitude, and 3) energy to produce strong welds. It was expected that excessively high energy, amplitude, and weld force would each increase the rate of internal heating at the faying surface, resulting in excessive squeeze flow and reduced weld strength. Results ranged from 1.6 to 31 N for peel strength testing, 0.05 to 5.6 MPa for shear strength, and 78 to 2,600 mN for tearing force.

The response variables were plotted as function of energy for each of the six materials. Spline curve lines were added in all of the graphs and are shown for visualization only. While they approximate the response as a continuous curve across energy levels, response data only exists at discrete energy values. All error bars correspond to one standard deviation with a population of four or five.

These results were then analyzed in JMP statistical software using 3-way Analysis of Variance (ANOVA) with replications to identify statistically significant relationships between the three single terms and four cross terms variables and the three response (dependent) variables (see Table 4). Effects test tables were created to determine the probability values, or p-values, for each independent variable. Low p-values, below the 0.05 level of significance adjusted for the total number of effects as shown in Equation (4), indicated that the means of the response variables were dependent on the explanatory variables.

Table 4 Seven main and interaction effects for benchtop welds

Main Effects	**Interaction Effects**
Energy	Energy and Amplitude
Amplitude	Energy and Weld Force
Weld Force	Amplitude and Weld Force
	Energy, Amplitude, and Weld Force

$$\alpha = \frac{0.05}{7} = 0.007 \qquad (4)$$

In addition, all results were analyzed in JMP to determine whether statistically significant relationships existed between the three single term and four cross term explanatory variables and the coefficient of variance, Equation (5), for each of the response variables. That is to say, statistical tests were conducted to determine if the independent variable affected the repeatability of the dependent variables. Effects tests tables were created to determine the p-values for each explanatory variable. P-values less than the adjusted level of significance, 0.007, indicate that the C_v of the response variable was dependent on the explanatory variables.

$$C_v = \frac{\sigma}{\mu} \qquad (5)$$

The test results for the coefficient of variance for peel strength and tear resistance were not found to be statistically significant and are not detailed. A discussion of the significant relationships between coefficient of variance for shear strength and the dependent variables is provided in the "Coefficient of Variance of Shear Strength Results" in the following section.

Peel Strength Results

The p-values for peel strength in Table 5 show evidence of a significant effect of amplitude on peel strength for F2A and YH materials, although this relationship is not clear in Figure 12 and Figure 17. Table 5 also shows an interaction effect of energy and weld force for peel strength for those materials. In more detail, the effects of energy and weld force were dependent on each other [13]. This can be seen by comparing the different slopes of the curves in Figure 12 and Figure 17. It is seen that the slope of the lines (peel strength as a function of energy) is higher at higher weld forces. This is likely the result of better coupling of the horn to the part at the higher forces, allowing better heating. In addition, the higher weld forces may have promoted better alignment between the horn and the anvil, in turn promoting more uniform welding. Because this higher energy and high force did not result in lower weld strength, it is suggested that no effects of excessive squeeze flow were seen and the energy and force levels were below the critical value that would promote this adverse effect.

The peel strength for materials F2B, F8, and PW were significantly affected by energy and weld force. These were not interaction effects. For these materials, peel strength was generally proportional to weld force and energy. The overall slope of the curves in Figure 13, Figure 14, and Figure 16 are very similar for each weld force level, unlike the previous plots of interaction effects. This suggests that higher energy and force levels promoted better fusion of the faying surfaces independently.

Again, this effect would be limited at higher levels as a result of excessive welding and burn through.

Table 5 also indicates a significant interaction effect between energy and amplitude for the CB material. In more detail, Figure 15 shows that the slope of peel strength as a function of energy appears to be dependent on amplitude (which is statistically supported). For example, in this case peel strength increased for the 400 J level as amplitude increased. This could be because higher amplitudes promoted more uniform welds (approaching the thickness of the film thickness) and the higher energy promoted better fusion. In more detail, at the high amplitude, the relative standard deviation (experimental error) is 25%, while at the lower energy and amplitude the relative standard deviation is as high as 50%. This is in agreement with the fact that higher amplitudes promote more uniform welds as long as the amplitude and energy are not excessive enough to promote burn through and weld or film damage.

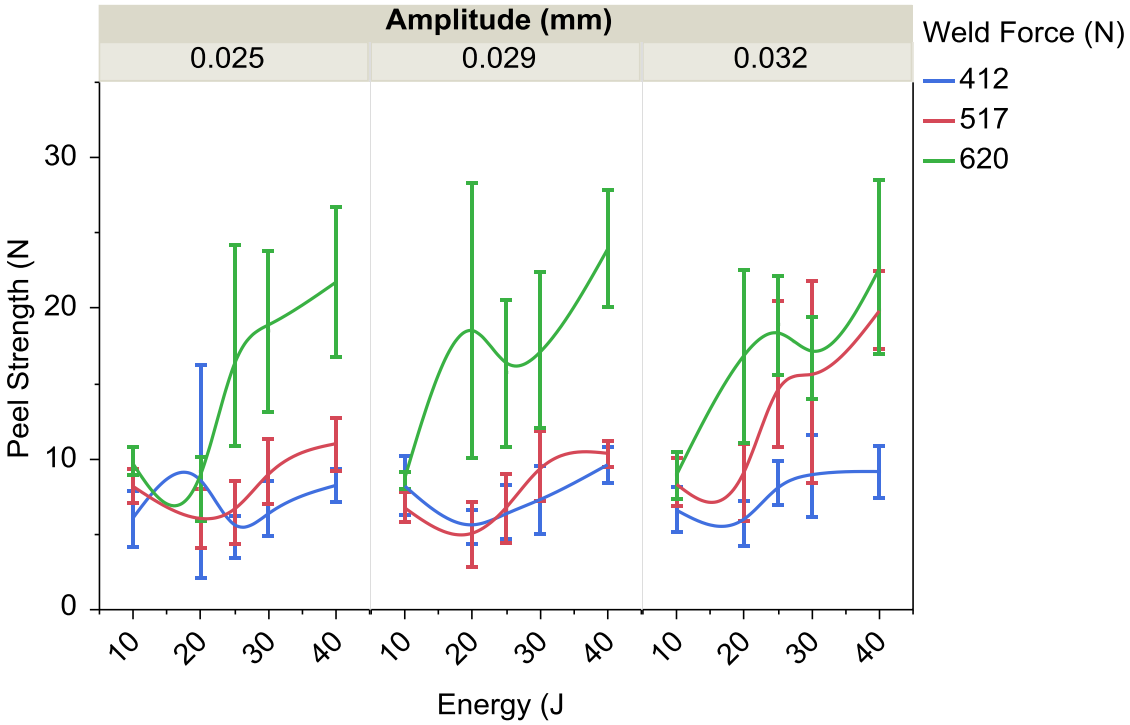

Figure 12 Peel strength (N) as a function of energy (J) for F2A

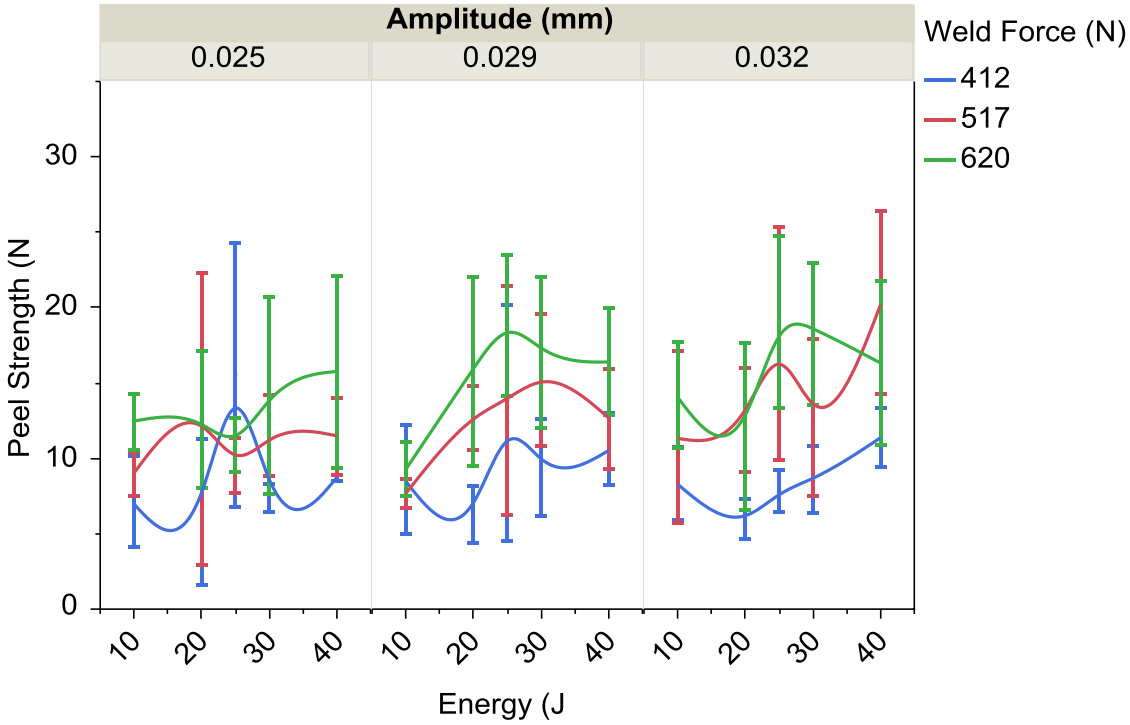

Figure 13 Peel strength (N) as a function of energy (J) for F2B

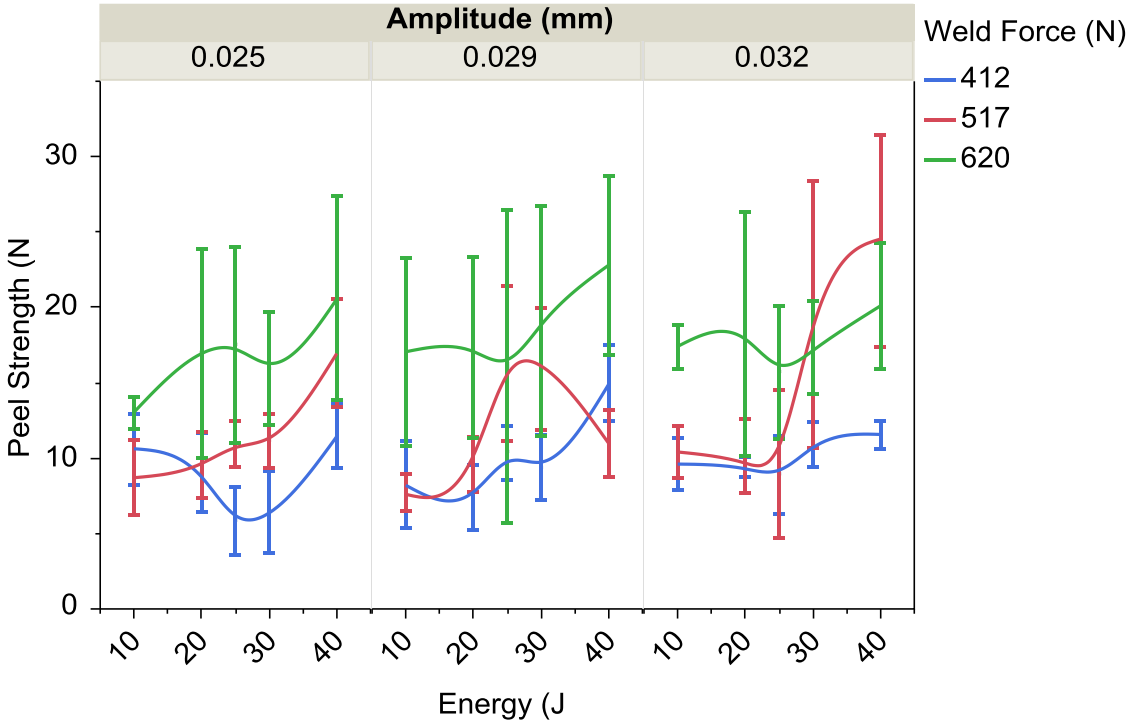

Figure 14 Peel strength (N) as a function of energy (J) for F8

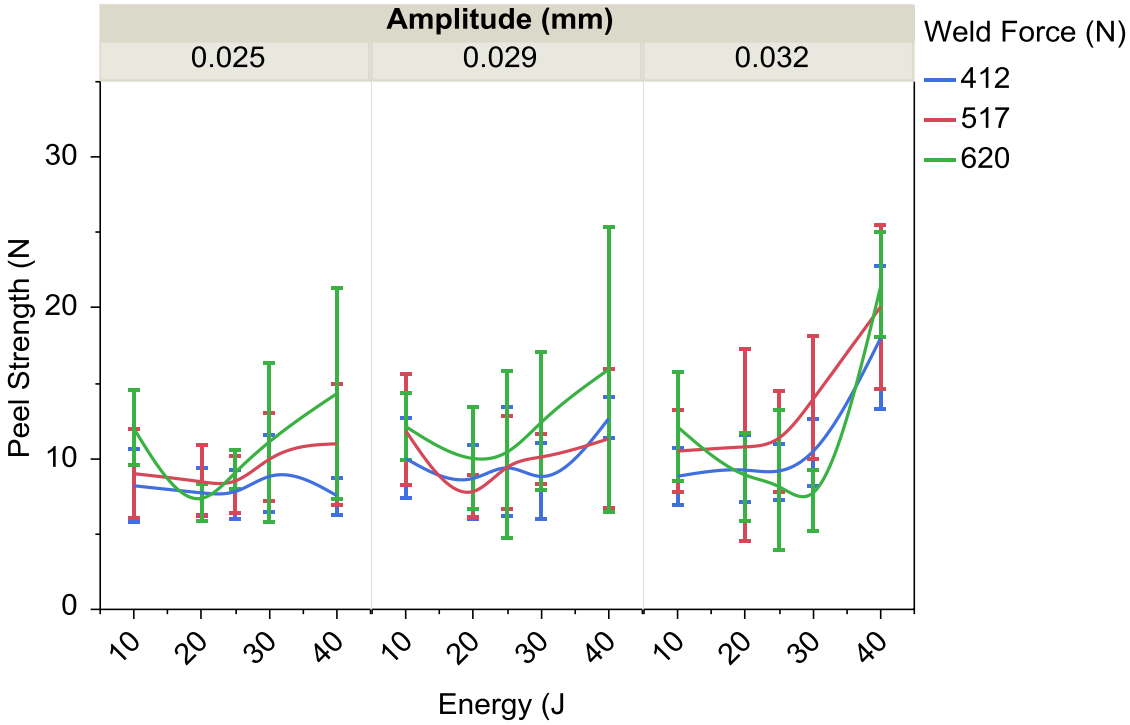

Figure 15 Peel strength (N) as a function of energy (J) for CB

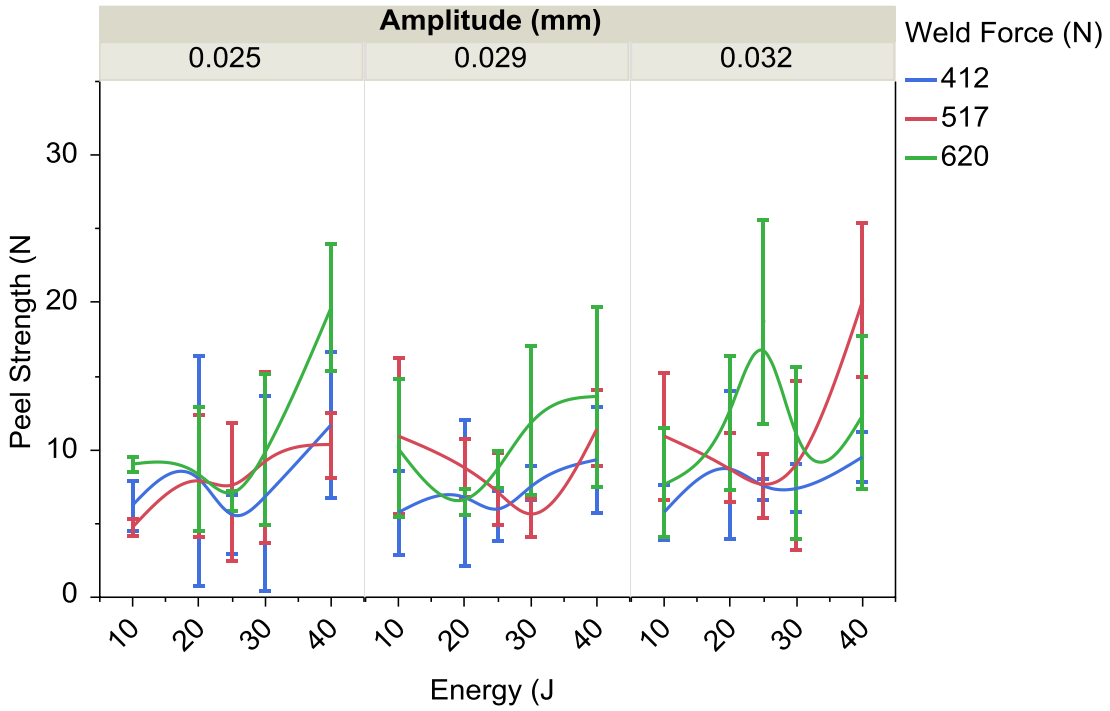

Figure 16 Peel strength (N) as a function of energy (J) for PW

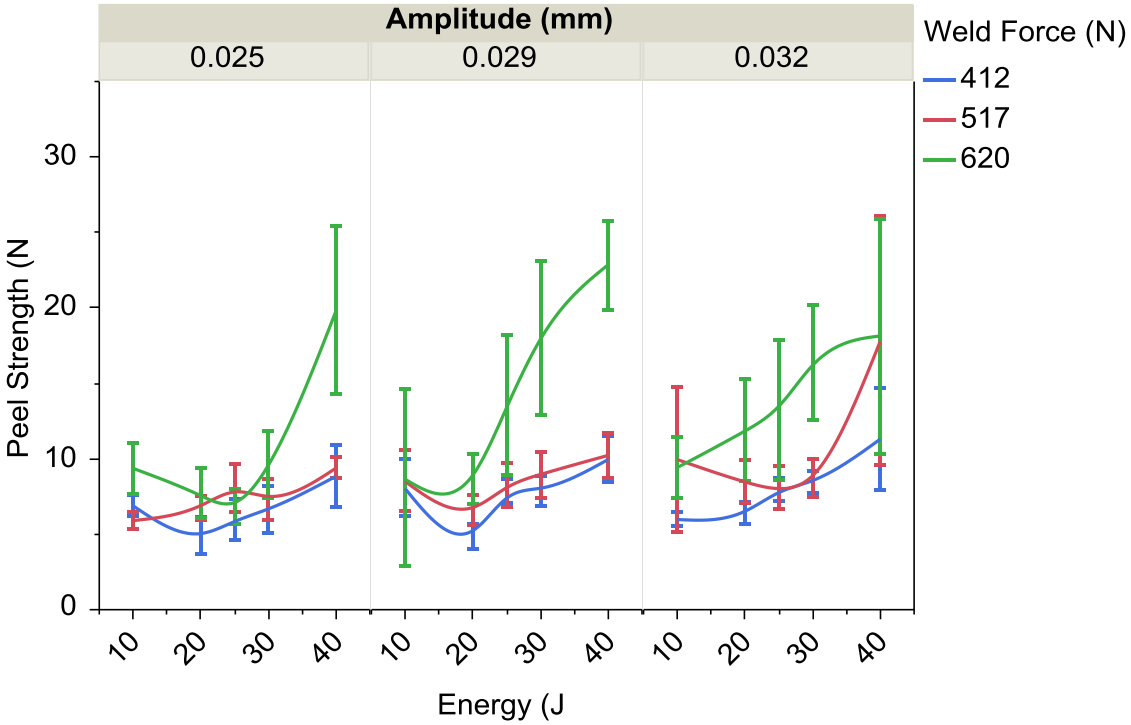

Figure 17 Peel strength (N) as a function of energy (J) for YH

Table 5 P-values for peel strength

Source of Variation	Material ID					
	F2A	F2B	F8	CB	PW	YH
Energy	<0.0001*	<0.0001*	<0.0001*	<0.0001*	<0.0001*	<0.0001*
Weld Force	<0.0001*	<0.0001*	<0.0001*	0.0090	<0.0001*	<0.0001*
Energy×Weld Force	<0.0001*	0.4882	0.2764	0.3208	0.2399	<0.0001*
Amplitude	0.0002*	0.0088	0.0123	0.0002*	0.0445	<0.0001*
Energy×Amplitude	0.1444	0.2642	0.3564	0.0005*	0.4469	0.1671
Weld Force×Amplitude	0.5683	0.0660	0.7528	0.1533	0.5367	0.1988
Energy×Weld Force×Amplitude	0.4164	0.8854	0.2386	0.5006	0.2920	0.3940

*p-value < α indicates significant difference in means

Shear Strength Results

Table 6 indicates a significant interaction effect between energy and weld force for shear strength for all materials. This is supported by Figure 18-Figure 23, where shear strength is generally inversely proportional to energy. In more detail, shear strength is relatively high for all weld forces at lower energy levels and low for forces of 517 and 620 N at the 300 and 400 J energy levels. It is believed that at the higher energy and force settings, the weld experiences burn through (which was visually observed) and excessive welding resulted in a loss in weld strength.

It is important to note that this was not seen in the peel strength test because here, the ultimate force at failure at the highest weld strengths was 26 to 31 N, while in the shear strength tests the ultimate forces were as high as 85 to 253 N. Thus, the effect of over weld was not seen in peel tests. This pattern was consistent across the

balance of the materials, with the exception of some high strength values at the mid-energy levels for materials F8 and PW.

Material F2A also exhibited a significant interaction effect between energy and amplitude. This can be seen in Figure 18, where shear strength is inversely proportional to energy as amplitude increases. Again, the reason for this loss in weld strength is probably related to over welding and the onset of burn through.

Materials F2B, CB, and YH also exhibited a significant relationship between shear strength and amplitude according to the p-values in Table 6. However, this is difficult to differentiate from Figures Figure 19Figure 21, and Figure 23.

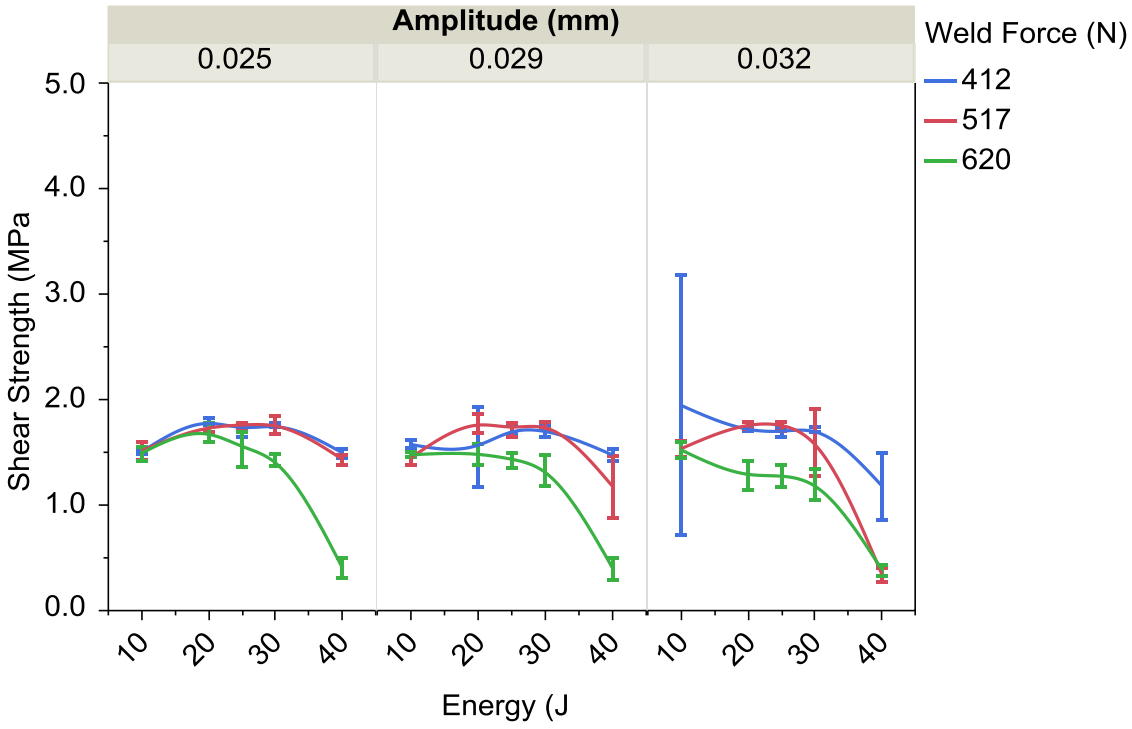

Figure 18 Shear strength (MPa) as a function of energy (J) for F2A

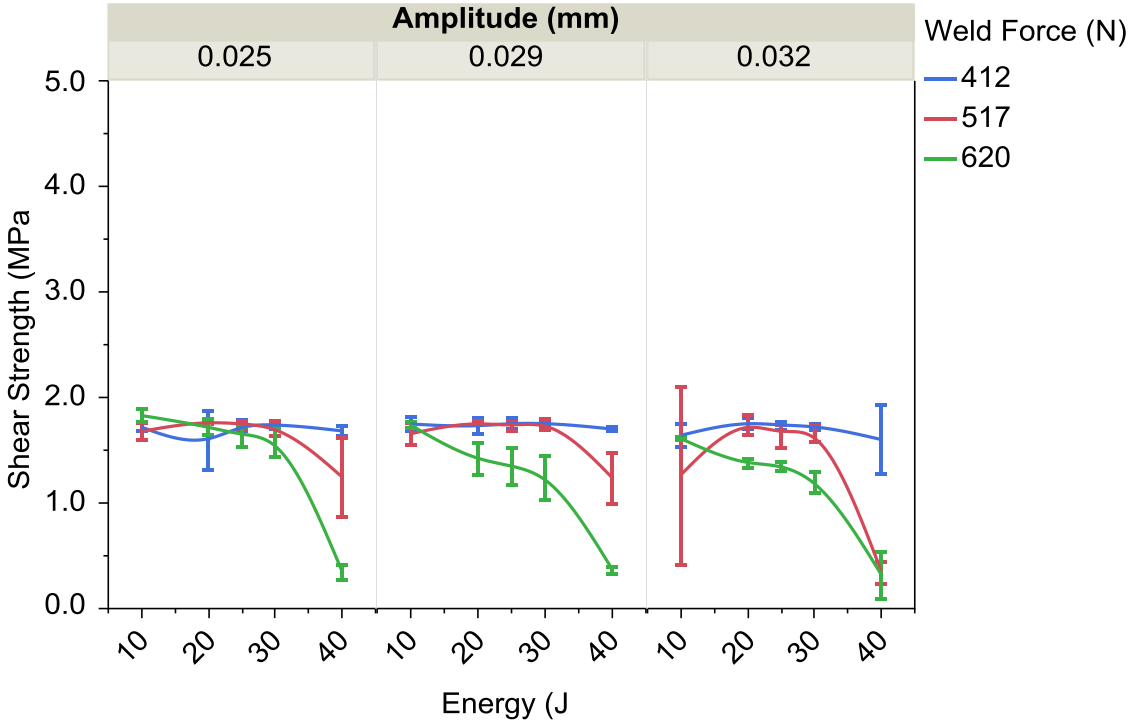

Figure 19 Shear strength (MPa) as a function of energy (J) for F2B

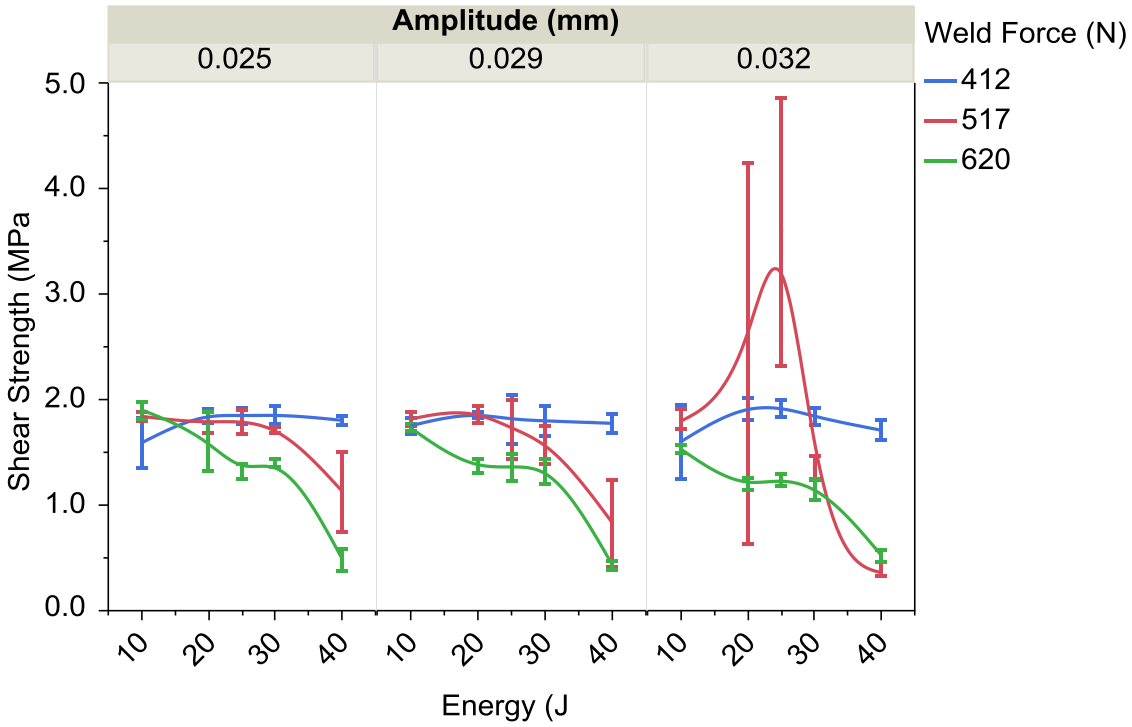

Figure 20 Shear strength (MPa) as a function of energy (J) for F8

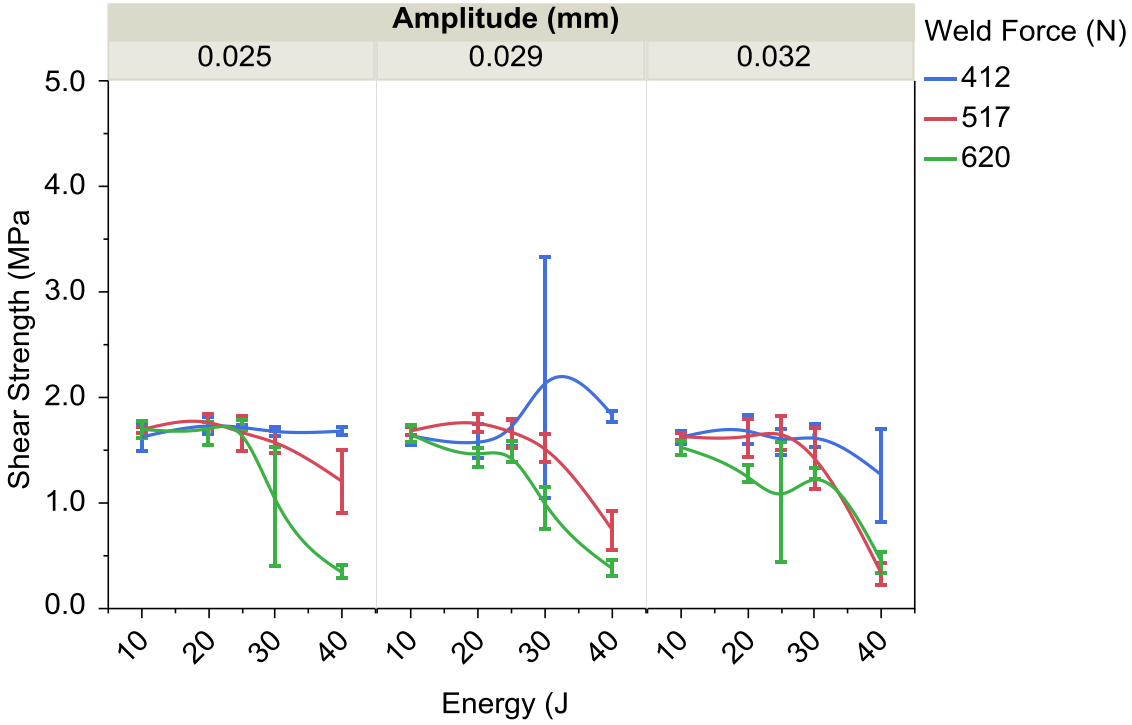

Figure 21 Shear strength (MPa) as a function of energy (J) for CB

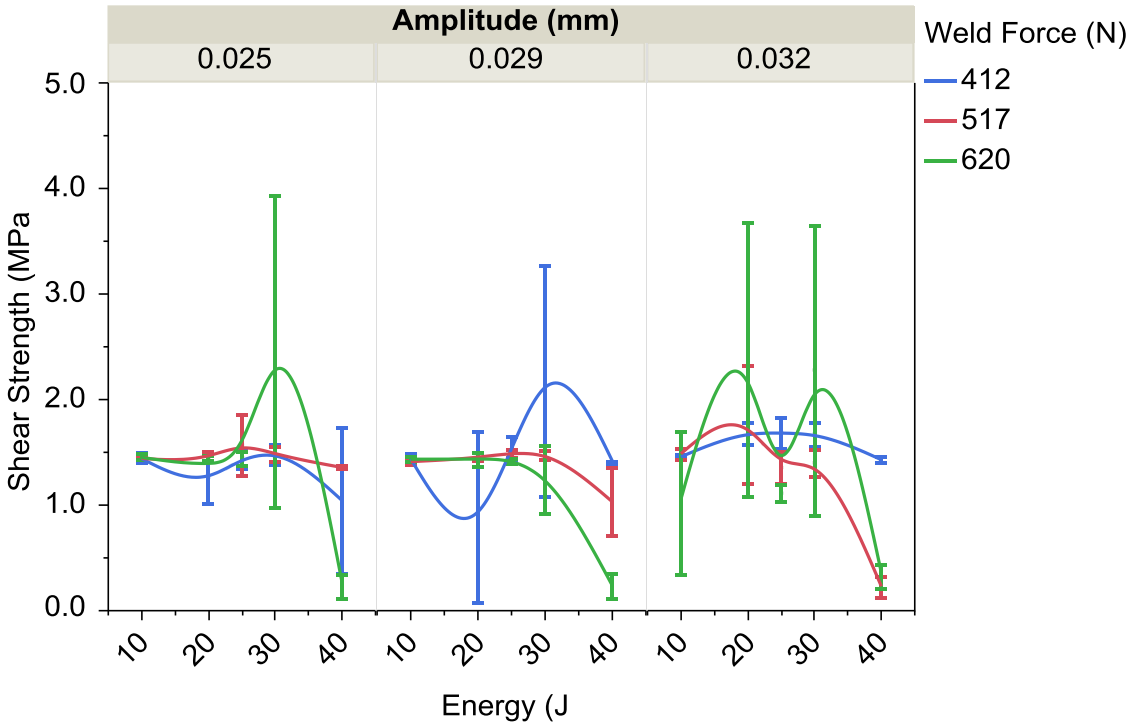

Figure 22 Shear strength (MPa) as a function of energy (J) for PW

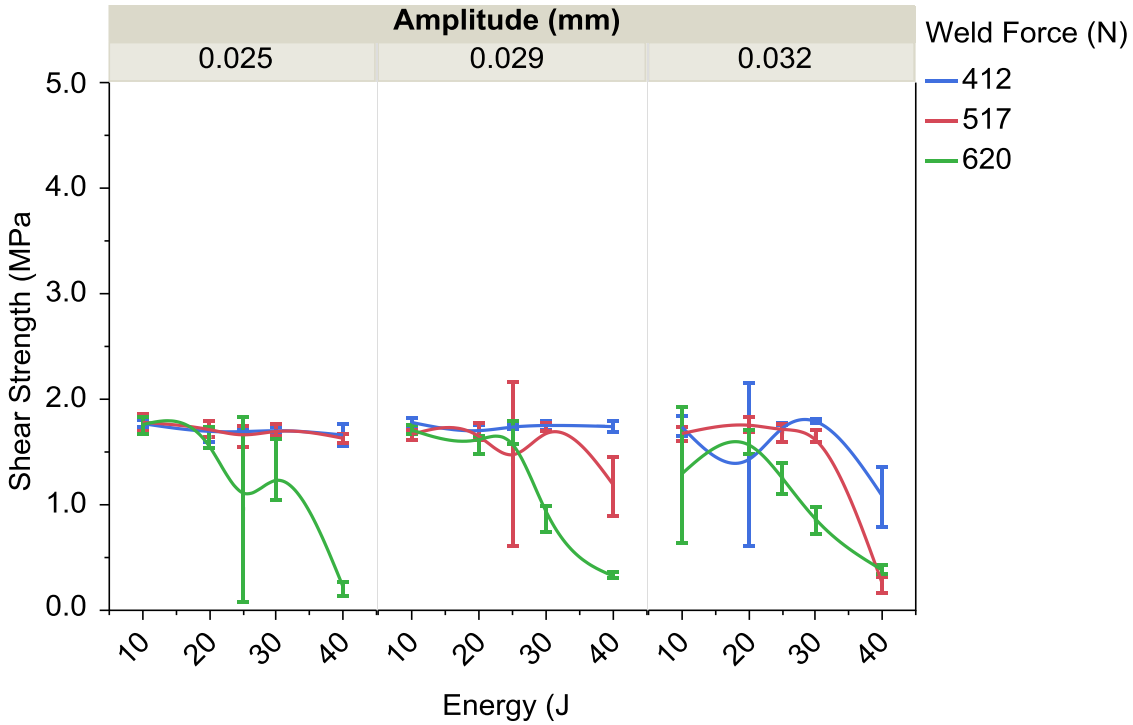

Figure 23 Shear strength (MPa) as a function of energy (J) for YH

Table 6 P-values for shear strength

Source of Variation	**Material ID**					
	F2A	F2B	F8	**CB**	**PW**	**YH**
Energy	<0.0001*	<0.0001*	<0.0001*	<0.0001*	<0.0001*	<0.0001*
Weld Force	<0.0001*	<0.0001*	<0.0001*	<0.0001*	0.1850	<0.0001*
Energy×Weld Force	<0.0001*	<0.0001*	<0.0001*	<0.0001*	0.0016*	<0.0001*
Amplitude	0.0095	0.0001*	0.8107	0.0009*	0.8359	0.0036*
Energy×Amplitude	0.0002*	0.2398	0.2999	0.1225	0.2967	0.0217
Weld Force×Amplitude	0.2647	0.0253	0.3415	0.7128	0.3828	0.5614
Energy×Weld Force×Amplitude	0.0847	0.5445	0.4641	0.0531	0.6800	0.0773

*p-value < α, indicates significant difference in means

Coefficient of Variance of Shear Strength Results

The p-values for the coefficient of variance of shear strength in Table 7 show evidence of a significant effect of energy for materials F2B, CB, and PW. This evidence is seen in Figure 24, Figure 25, and Figure 26. The figures show that the coefficient of variance is proportional to energy. It is believed that there is a critical energy value of 300 J at which point burn through may start to occur. When burn through is initiated, the effects of excessive heating compound the burn through, resulting in a wide range of weld strengths. In some cases, the burn through did not initiate, and relatively strong welds were produced. These two possible outcomes resulted large experimental error. This compounding effect is most likely caused by excessive heating resulting in a disproportional increase in loss modulus, resulting in thermal "run away" [6].

Table 7 also indicates significant p-values for the effect of weld force and the interaction effect of energy, weld force, and amplitude on the C_v of shear strength for material YH. All three explanatory variable effects on C_v were dependent on each other. This can be seen in Figure 27. For example, at low amplitude and low energy, the shear strength C_v is low for all weld forces. At higher amplitudes, the C_v increases at the higher energies for the lower weld forces. It is seen that the highest weld force, lowest energies, and highest amplitude had the most variance. Again it is believed that at higher energy and amplitude values, there were critical values, that once exceeded, resulted in possible over welding, and once initiated, the processes

would promote excessive over welding. However, it is clear that in all cases higher weld force resulted in higher variance.

Excessive squeeze flow and burn through is more likely to occur at high energy and high weld force levels compared to lower energy and weld force levels. Along with burn through, inconsistencies occur in the weld diffusion zone, which lead to more variation in weld strength.

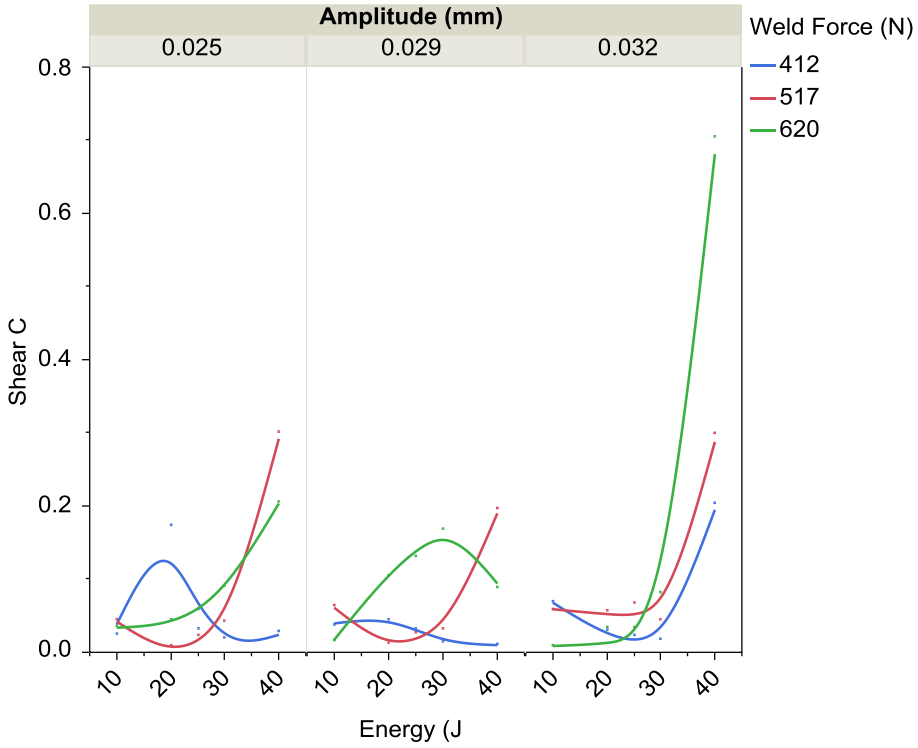

Figure 24 C_v of shear strength as a function of Energy (J) for F2B

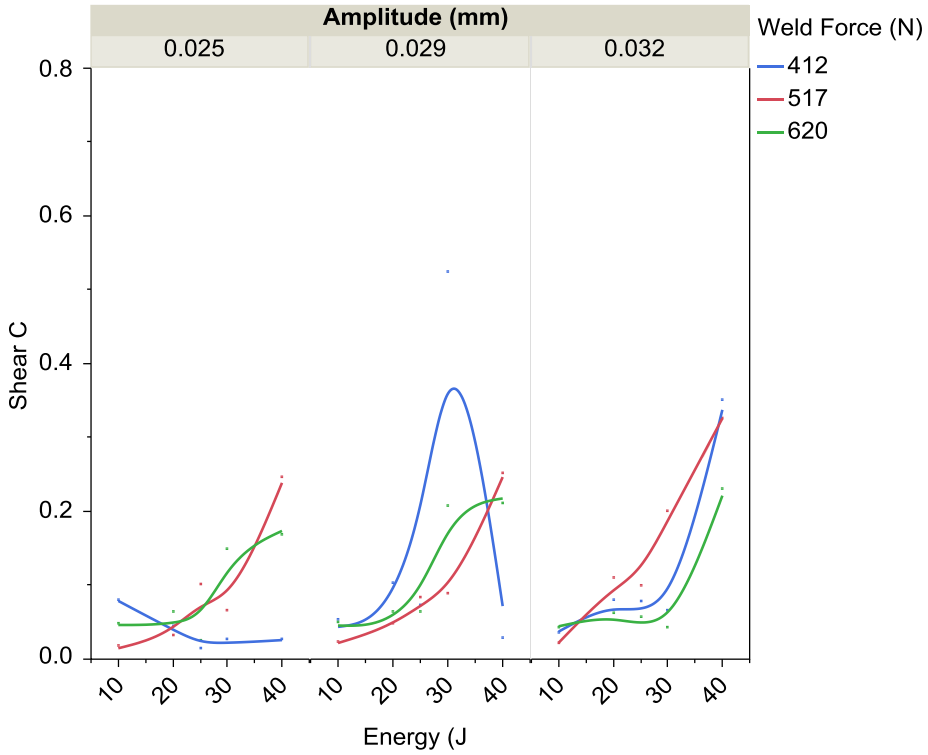

Figure 25 C_v of shear strength as a function of Energy (J) for CB

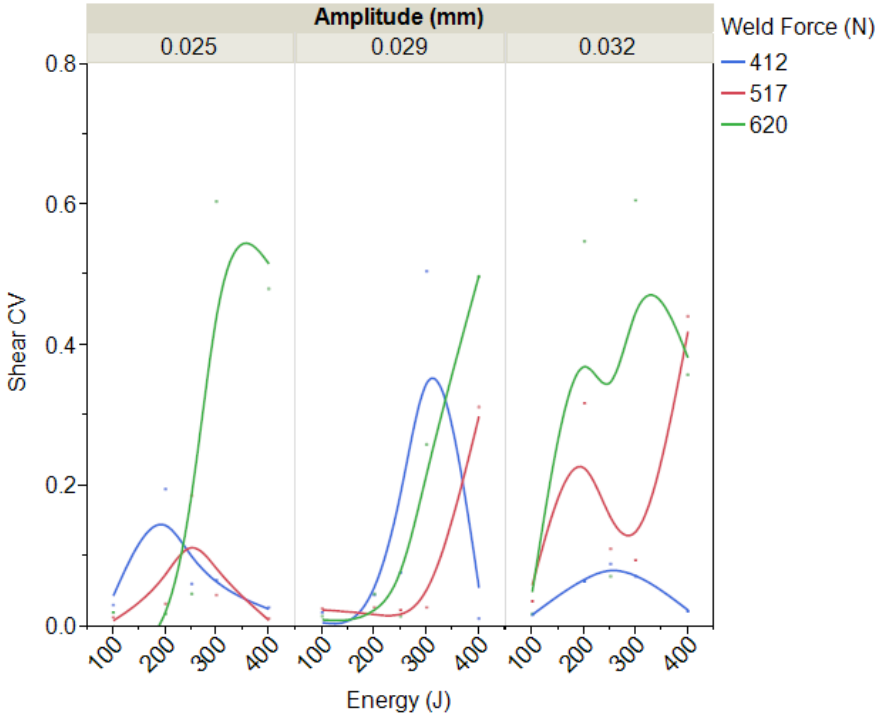

Figure 26 C_v of shear strength as a function of Energy (J) for PW

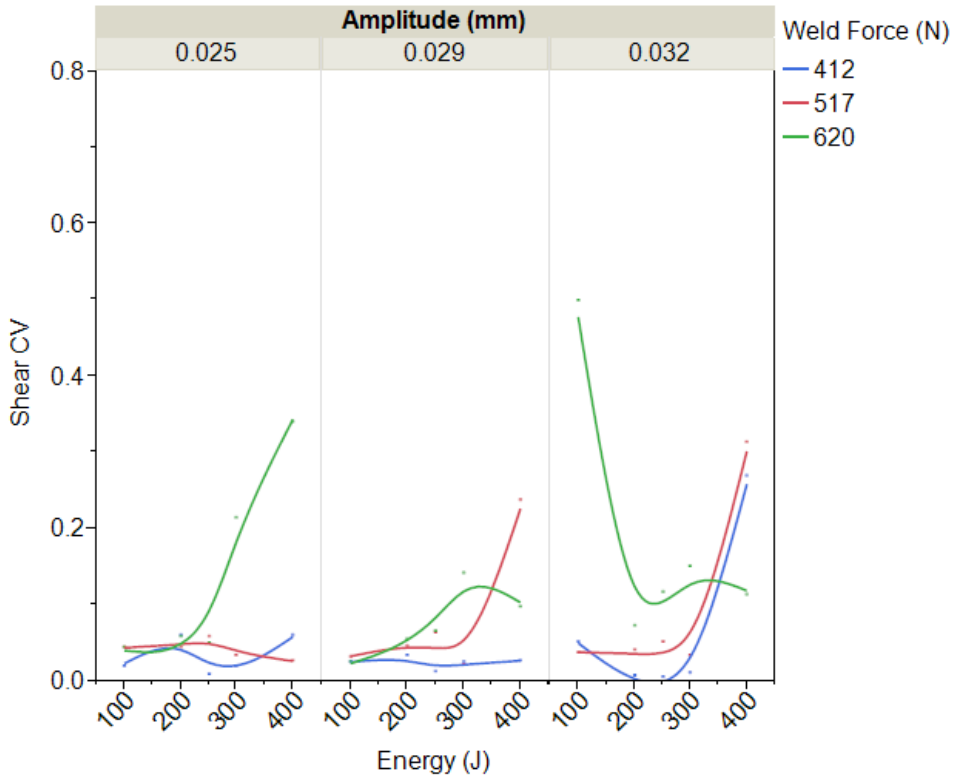

Figure 27 C_v of shear strength as a function of Energy (J) for YH

Table 7 P-values for coefficient of variance for shear strength

Source of Variation	**Material ID**					
	F2A	F2B	F8	**CB**	**PW**	**YH**
Energy	0.2566	0.0003*	0.2445	<0.0001*	0.0019*	0.0425
Weld Force	0.8713	0.0493	0.8381	0.8364	0.0096	0.0040*
Energy×Weld Force	0.0156	0.0089	0.2754	0.5810	0.0132	0.6158
Amplitude	0.0489	0.2874	0.3141	0.1312	0.2522	0.1717
Energy×Amplitude	0.5692	0.0805	0.4225	0.1259	0.8371	0.4831
Weld Force×Amplitude	0.0877	0.3883	0.6256	0.2439	0.5012	0.9164
Energy×Weld Force×Amplitude	0.3763	0.2605	0.9985	0.2014	0.4395	0.0013*

*p-value < α, indicates significant difference in means

Tear Resistance Results

Materials F2A and F2B both exhibited a significant interaction effect between energy and amplitude as seen in Table 8. In more detail, Figure 28 and Figure 29 show tearing force is generally inversely proportional to energy increases at the lower amplitude setting. However, it is generally proportional to energy at higher amplitude settings. This pattern is slightly more obvious for the F2A material. It is believed that these observations are related to a balance of over welding (burn through) as well as sufficient fusion to produce a relatively strong weld. It is important to note that there is significant experimental error (large error bars), which is typical of tear testing results.

Material F2B also showed an interaction effect for weld force and amplitude. Figure 29 shows moderate and flat tearing force across amplitudes for the two low weld forces and increasing tearing force over amplitudes at the highest weld force. This can likely be explained by brittleness caused by burn because of excessive squeeze flow at higher amplitudes and weld forces.

Weld force was also a significant main effect for F2A, F2B, F8, and PW as indicated in Table 8. For the PW material, shown in Figure 32, low weld force resulted in higher weld strength. This is incongruent with the other five materials, but within the range of being explained by experimental error. Figure 30 show the tearing force being consistently proportional to high weld force, especially at the 200 to 300 J energy levels. This suggests that at these levels there is likely better coupling of the horn to the part, allowing better heating and better alignment

between the horn and the anvil, in turn promoting more uniform welding. Tearing force decreased at the 400 J level which is believed to be an indication of excessive squeeze flow and over weld conditions resulting in lower strength.

Amplitude was the only significant main effect for material YH indicated by Table 8. Tearing force is slightly higher across all energies and weld forces at the highest amplitude (Figure 33). This may be explained by the fact that higher amplitudes promoted more uniform welds (approaching the thickness of the film thickness).

There were no significant effects for material CB, as shown in Table 8 and Figure 31.

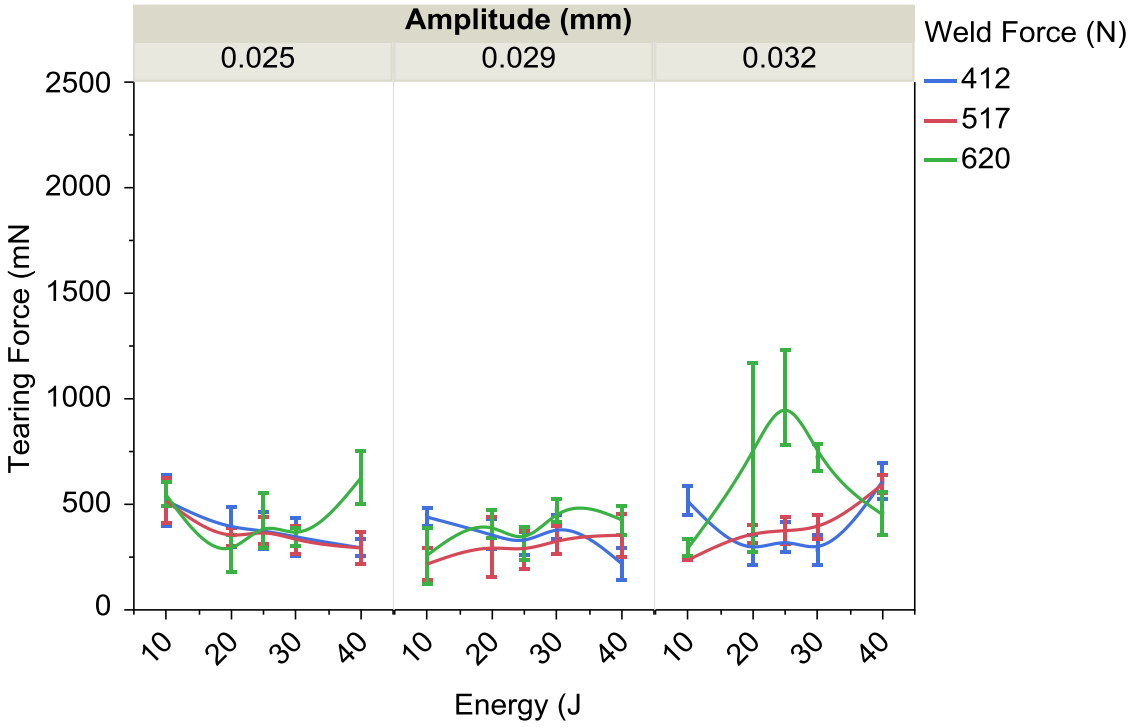

Figure 28 Tearing force (mN) as a function of energy (J) for F2A

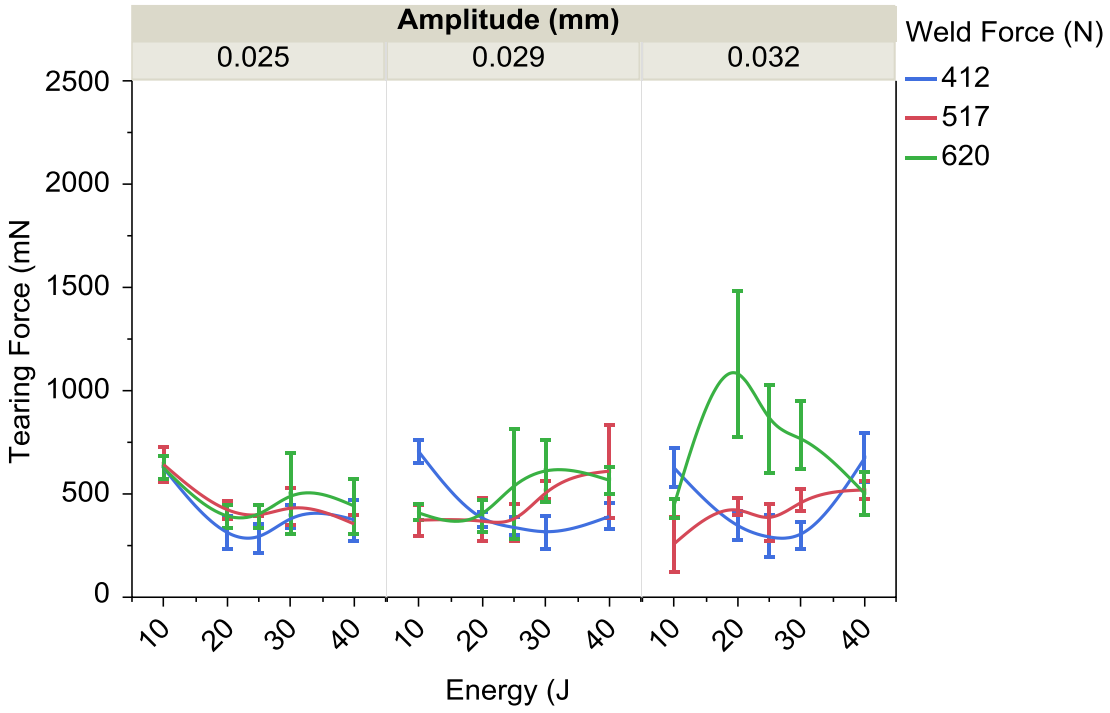

Figure 29 Tearing force (mN) as a function of energy (J) for F2B

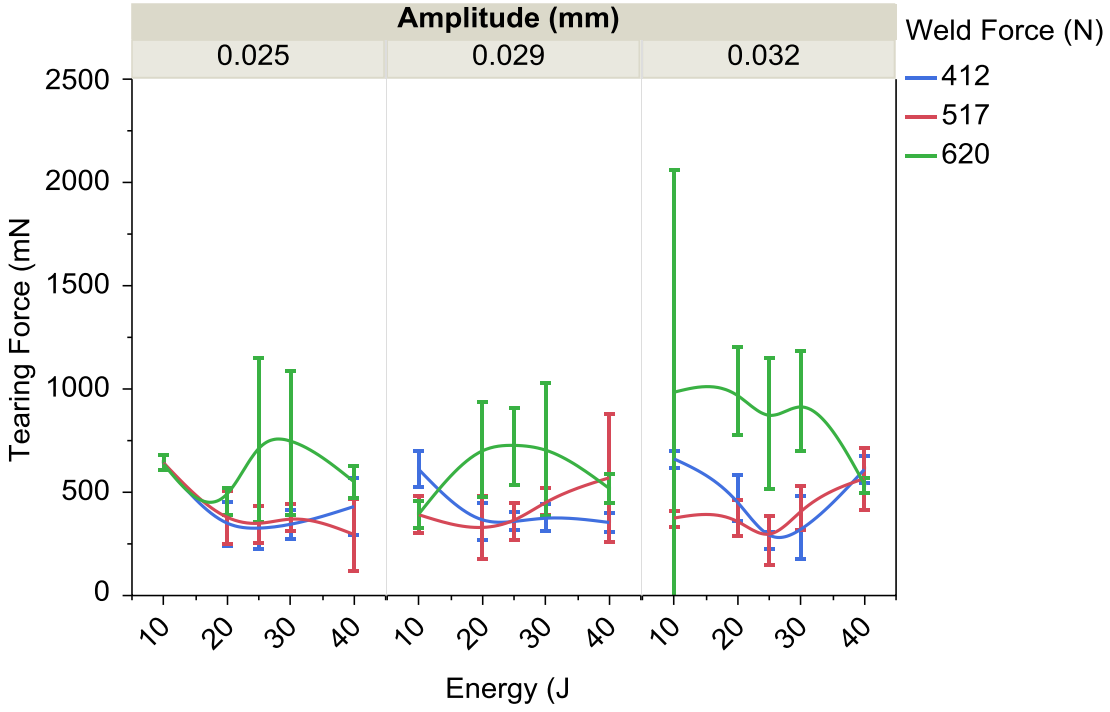

Figure 30 Tearing force (mN) as a function of energy (J) for F8

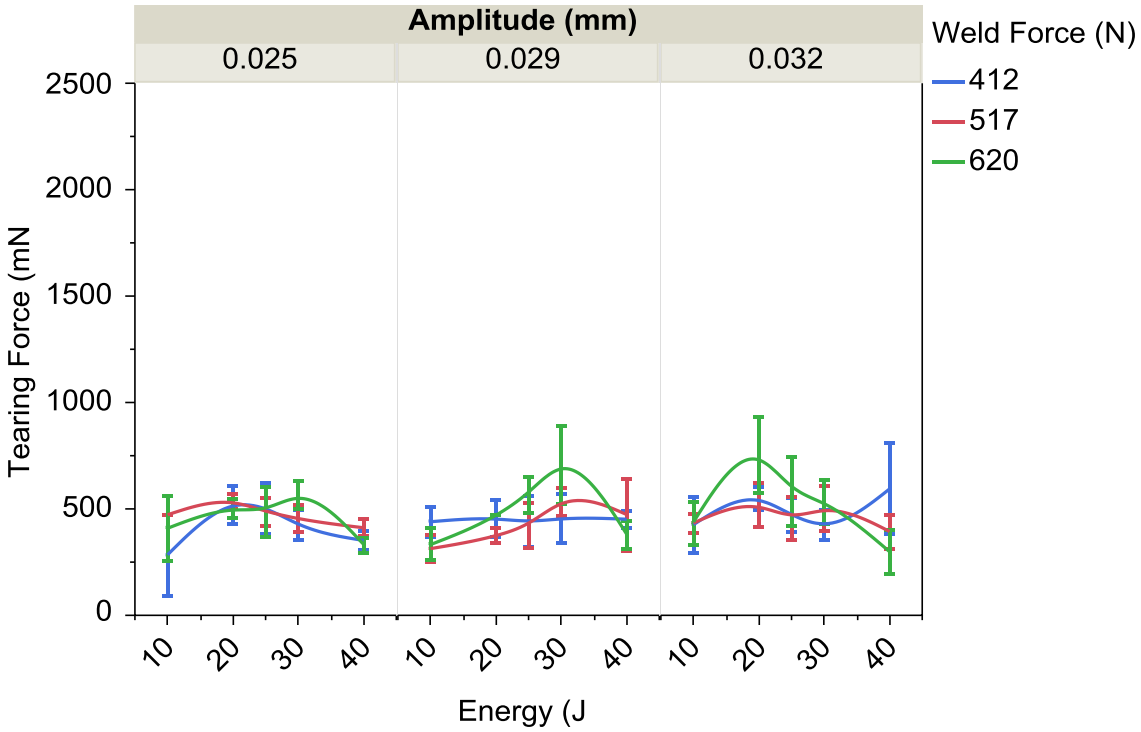

Figure 31 Tearing force (mN) as a function of energy (J) for CB

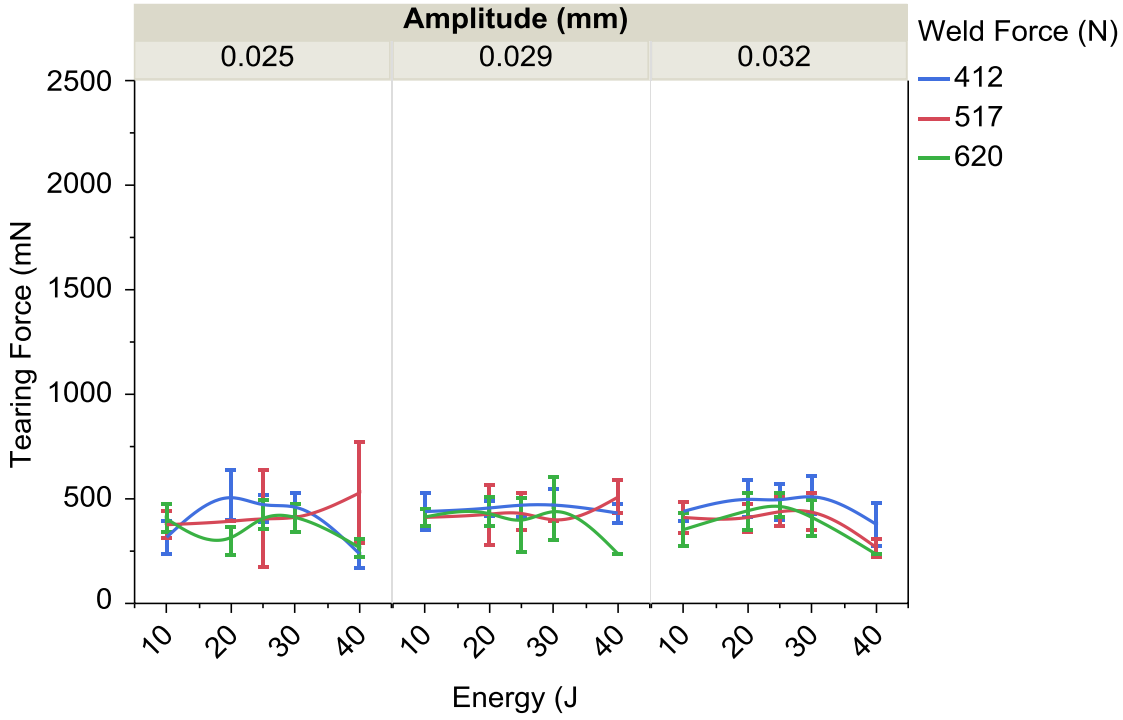

Figure 32 Tearing force (mN) as a function of energy (J) for PW

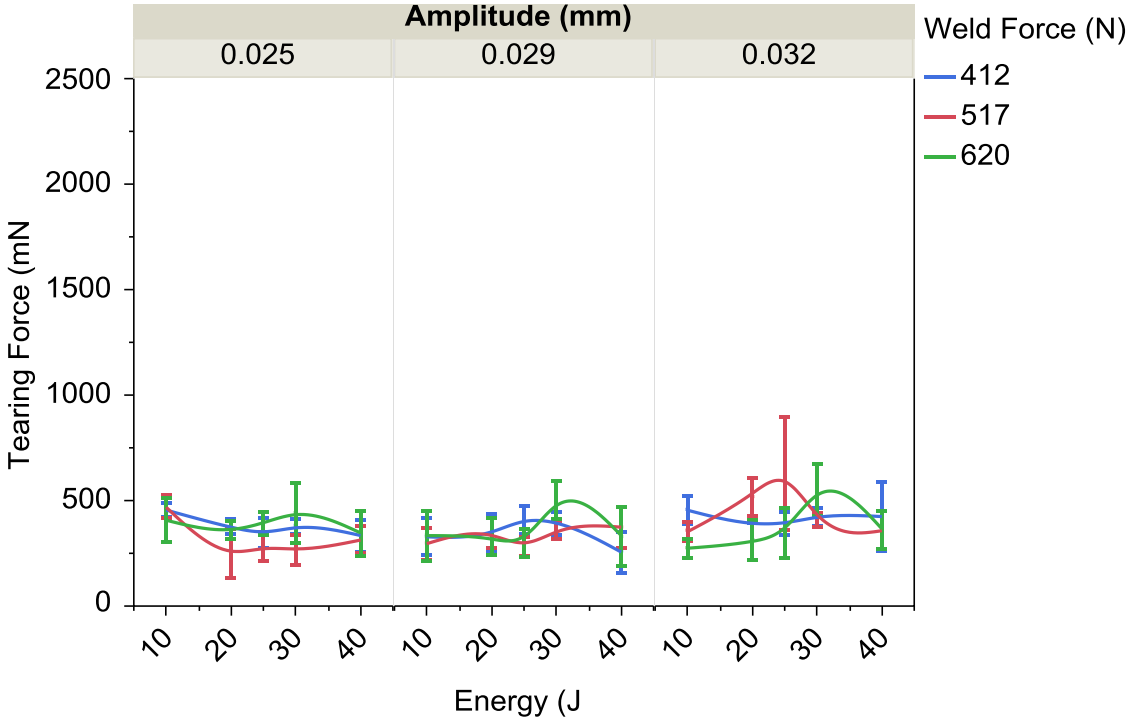

Figure 33 Tearing force (mN) as a function of energy (J) for YH

Table 8 P-values for tearing force

Source of Variation	**Material ID**					
	F2A	F2B	F8	**CB**	**PW**	**YH**
Energy	0.3968	0.2597	0.0565	0.8662	0.0228	0.5300
Weld Force	<0.0001*	<0.0001*	<0.0001*	0.0664	0.0002*	0.6702
Energy×Weld Force	0.0073	0.0722	0.5359	0.0625	0.0720	0.0525
Amplitude	0.0068*	0.0016*	0.0303	0.0548	0.2091	0.0068*
Energy×Amplitude	0.0008*	0.0028*	0.5107	0.8570	0.0686	0.0185
Weld Force×Amplitude	0.0150	0.0058*	0.1183	0.8999	0.4163	0.1993
Energy×Weld Force×Amplitude	0.1786	0.5363	0.1000	0.2166	0.7200	0.6183

*p-value < α, indicates significant difference in means

Conclusions

The aim of this study was to identify the set of parameters that yielded the highest weld strengths. Three explanatory variables (independent)—energy, amplitude, and weld force—were investigated to determine whether any of them had a significant effect on peel strength, shear strength, or tearing force as well as the effect of the independent variables on the experimental error. All three explanatory variables were expected to have an inversely proportional relationship with weld strength.

Results for all six materials were analyzed to determine whether a set of parameters resulted in high peel strength, shear strength, and tear resistance simultaneously. It as was seen that the 0.032 mm amplitude and 620 N weld force resulted in relatively high peel and shear strength as well as tear resistance for the majority of the materials. There was no single energy level that resulted in relatively high weld strengths for all responses. The 400 J level resulted in the highest peel strength welds for all materials, the 300 J setting had high shear strength outputs for half of the materials, and the highest tear resistance was recorded most often at the 200 J level. In general the optimized weld parameters for all three response variables, would be an amplitude of 0.032 mm, weld force of 620 N, and weld energy of 300 J.

The highest peel strength was found at high weld forces and high energies for all materials, and for select materials, high amplitudes resulted in even higher peel strength. Energy and weld force were significant factors for almost all materials.

Because higher energy and high force did not result in lower weld strength, it is suggested that the effects of excessive squeeze flow were not seen and the energy and force levels were below the critical value that would promote this adverse effect despite visual evidence of over weld. It is possible that the displacement of the metallized layer caused an exaggerated appearance of over weld.

All independent variables were significant for different materials with respect to tear resistance. For the F2A, F2B, F8, and CB materials, the highest tear resistance was the result of high force, high amplitude, and mid-range energies, although none of the variables were statistically significant for the CB material. The YH material was strongest at higher amplitudes as well as mid-range force and energy levels. Despite having a statistically significant dependence on energy, results for the PW were largely indistinguishable.

Both energy and weld force had significant effects on shear strength. For most combinations, results for shear strength did reflect the study predictions with the highest levels of shear strength recorded at the low energy and weld force levels. This may be because the shear strength trials had the least dramatic failures of the three analyses. Peel strength test specimens often exhibited signs of the layers pulling apart from each other (delamination), and the material was also known to break at the weld rather than peeling apart. Tear specimens sometimes tore obliquely or broke along the weld. Those volatile failure modes were audibly noisier than when a specimen tore or peeled cleanly. The sound that accompanied a failure was a release of energy, and that sudden release came as a result of being subjected

to maximum load. Further analysis could be completed in order to attempt to correlate the categorical failure mode with the explanatory variables and perhaps also the response variable to determine whether there was an additional relationship that had not yet been considered.

In addition, all results were analyzed to determine whether statistically significant relationships existed between the independent variables and the coefficient of variance for each of the response variables. The tests were not found to be statistically significant for peel strength or tear resistance; however, energy, weld force, and an interaction effect between energy, weld force, and amplitude were found to be significant sources of variation for several of the materials. It is believed that some combinations of these parameters resulted in excessive heating. In this instance, over weld occurred and welds were weak. If this did not occur, strong welds were created consistently.

CHAPTER 3. PEEL STRENGTH OF COEXTRUDED POLYOLEFIN BAGS CREATED IN A VERTICAL FORM, FILL, SEAL MACHINE WITH ULTRASONIC END SEALS

Modified from a paper to be submitted to *Packaging Technology and Science*

J. Riedl, D. Grewell, D. R. Raman[1], M. Kessler[2]

Abstract

The peel strength of welds created on a vertical form, fill, seal (FFS) machine fitted with an ultrasonic horizontal end sealer was investigated in this study. Six different proprietary triple-layer, coextruded polyolefin films were tested over a number of machine settings, including two production rates, three energies, and three amplitudes. The aim of this study was to identify the set of parameters that yielded the highest weld strengths for the both top and the bottom end seals.

It was observed that low energy and amplitude resulted in relatively high strength for the top weld of one material and low production rate resulted in high strength for the top weld of two materials as well as in the bottom weld for two materials. The peel strength for the fifth material was directly proportional to energy, and data for the sixth material were inconclusive.

---

[1] Department of Agricultural and Biosystems Engineering, Iowa State University, Ames, Iowa 50010
[2] Department of Materials Science and Engineering, Iowa State University, Ames, Iowa 50010

Introduction

This research focuses on optimizing the strength of the end seals of bags made from six polyolefin films. Among other applications, bags of this type are commonly used to provide air, water, and chemical barrier packaging for foods such as potato chips. The industry standard for packaging such free-flowing products is using a FFS machine.

In a FFS machine, a roll of packaging film is placed on a reel and fed through a series of rollers that align and provide tension to the material. The film is fed around a forming shoulder as shown in Figure 34. A tube of film is created by a vertical fin or overlap seal usually made with a heat bar. The end sealing jaws closes, and two horizontal seals are made simultaneously. The upper seal forms the bottom for the bag being created in this cycle. The product to be packaged is dropped from a hopper down the tube into the bag. The film is advanced downward, and the end sealing jaws are activated again to create the top horizontal seal of the current bag as well as the bottom seal for the next bag above it. Finally, a blade slices between the top and bottom seals and the next cycle begins [3].

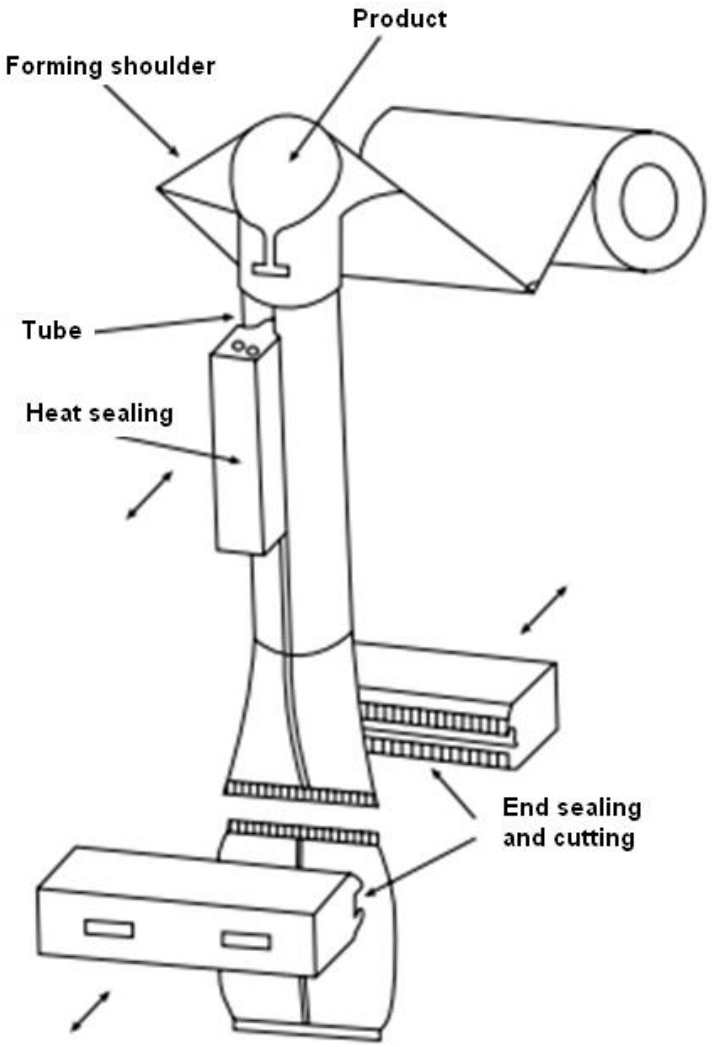

Figure 34 Schematic of vertical form, fill, seal machine [3]

The welds investigated in this study were created in a FFS machine equipped with ultrasonic end sealing, pneumatically controlled actuators. Similar to the study with the bench top plunge weld systems, weld quality can be controlled by varying standard ultrasonic machine factors such as horn size and shape, anvil size and shape, amount of energy delivered, amplitude, and frequency of vibration. However, additional process factors unique to producing bags also influenced weld strength. These process factors include, but are not limited to, production rate, open and close

rates of the end seal actuators, and machine timing factors. All process steps in a FFS system are timed by a virtual cam system. One cycle is represented by the virtual cam rotating through 360°. All process steps during a cycle start and stop at certain set points identified by degree. These processes include, but are not limited to, film advance, vertical seal, end seal, ultrasonic activation, and cool.

Screening Experiments

It is critical to identify a suitable combination of weld parameters in order to meet all design requirements and optimize the packaging process. Several sets of preliminary bags were created at Branson Ultrasonics Corporation (BUC) (Danbury, CT) from December 17-20, 2012 to identify the boundaries of an experimental design space to be investigated in more detail. Parameters examined in these screening experiments included production rate, ranging from 20 to 120 bags per minute (bpm), end seal start from 130° to 170°, energies from to 300 to 1800 J, and the entire range of allowable amplitudes from 0.016 to 0.032 mm.

Bags created using this broad set of screening parameters were inspected visually for puckering or folds, as these would likely be unsatisfactory to a customer. In order to determine whether the chosen machine parameters created airtight seals, these early specimens were subjected to burst and vacuum testing.

Burst testing was performed using a TM Electronics (Boylston, MA) BT Integra-Pack© test instrument. A needle was inserted into a bag and sealed to the bag with an adhesive O-ring as shown in Figure 35. Air was pumped into the bag through the needle and pressurized to 15.8 kPag. The machine measured pressure

drop and readings from 0% (no drop) to 50% drop were considered acceptable. Several bags were tested for the broad range of parameters described earlier and no bags passed the test. In most cases, a tear propagated where the needle penetrated the bag and created a leak. This test methodology was determined to be insufficient to detect leaks.

Figure 35 (Left) Burst test needle; (Right) Tear propagation at needle location

Figure 36 Vacuum chamber with specimen, lid, hose, and vacuum pump

Vacuum testing was then conducted to ensure that the sealing method provided the required airtight seals. Bags were placed into a vacuum chamber filled to approximately 3/4 with water. A plastic container with holes in the bottom was placed below the lid of the chamber to ensure the bags remained submersed. A small hose connected a hole in the lid of the chamber to a vacuum pump, all shown in Figure 36. The pump produced a 550 mmHg vacuum which was held for 20 seconds. Again, many of the tested bags leaked. Upon further inspection, independent of energy and amplitude settings, the welds exhibited systematic over weld in the top right corner and under weld in the bottom left corner relative to the FFS machine as shown in Figure 37.

Several attempts were made to better align the anvil; however, little success was achieved in producing more uniform welds. Also, it was not possible to adjust the regulator on the pneumatic line going to the end seal control because of machine design. In order to address this problem, representatives at BUC decided to replace the pneumatically controlled end seal actuators with actuators driven by servo motors. End seal jaws, shown in Figure 38, with servo motors provided more precise control of angular positioning than those with pneumatic actuators. This resolved the uniform heating issues.

Figure 37 Locations prone to over weld and under weld

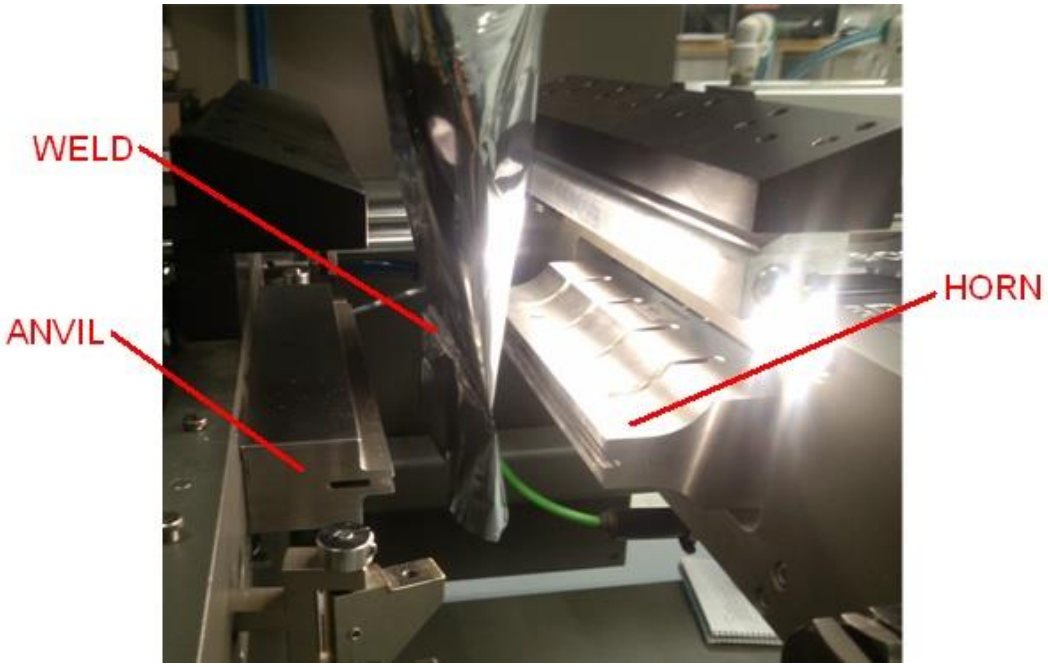

Figure 38 FFS machine equipped with ultrasonic horizontal sealer

A second set of preliminary bags was created at BUC on April 8-9, 2013, starting with the same parameters used in December 2012, production rates ranging from 20 to 120 bags per minute (bpm), end seal start from 130° to 170°, energies from to 300 to 1800 J, and the entire range of allowable amplitudes from 0.016 to 0.032 mm.

However, slow production rates (20 to 60 bpm) were eventually excluded from further investigation because any rate significantly lower than the industry standard of 100 bpm would likely not be accepted by a potential customer. Screening experiments showed that for the 80 to 120 bpm production rates an end seal start of 150° (on a 360° rotor) and greater was too late in the cycle for smooth machine operation. The 120 bpm speed was ultimately eliminated because the high coefficient of friction of the material caused bunching around the end seal and poor bag quality. In addition, it was seen in screening experiment specimens that the ultrasonic power supply did not have enough time in the fast cycle time to deliver energies as high as 1800 J. The highest peak energy delivery reported was only 853 J.

Creating high quality end seals at state-of-the-industry production rates was a key design requirement for this system. Therefore, the final set of experimental parameters for this study comprised two production rates of 80 and 100 bags per minute (bpm), a constant end seal start at 130°, three energies ranging from 300 to 900 J, and the entire range of allowable amplitudes from 0.016 to 0.032 mm as shown in Table 9. Other processing factors such as frequency, weld force, and

machine timing were held constant. There were 18 total treatments in the full factorial experimental design and five bags of each of the six materials were made each treatment, resulting in a total of 540 bags.

Table 9 FFS machine design of experiment

Factors	**Levels**
Energy (J)	900
	600
	300
Amplitude (mm)	0.032
	0.024
	0.016
Production Rate (bpm)	100
	80

Both weld energy and amplitude were expected to directly impact weld strength, which is inversely proportional to squeeze flow [6]. While the intuitive choice of very low process parameters will avoid excessive squeeze flow, interfacial healing is critical. Therefore, the lowest sealable energy and amplitude settings were used at the highest feasible speed because industry would be interested in increased production. The objective of this study was to identify the set of parameters that yielded the highest weld strength.

Experimental Procedure

All welds for this study were produced at Branson Ultrasonics Corporation (Danbury, CT) April 9-11, 2013, using a FFS machine equipped with a 30 kHz Branson 2000 DCX power supply and 2000X balun stack. The stack consisted of a

two transducers with balun (balancing transformer), two boosters, and one horn. In the balun system, two transducers were energized in parallel, shown in Figure 39, to drive the large horn without significant heat losses in order to protect the piezoelectric material inside. The balancing transformer ensures that each transducer operated at the same amplitude, in phase, despite the manufacturing and material variances between the two converters [14].

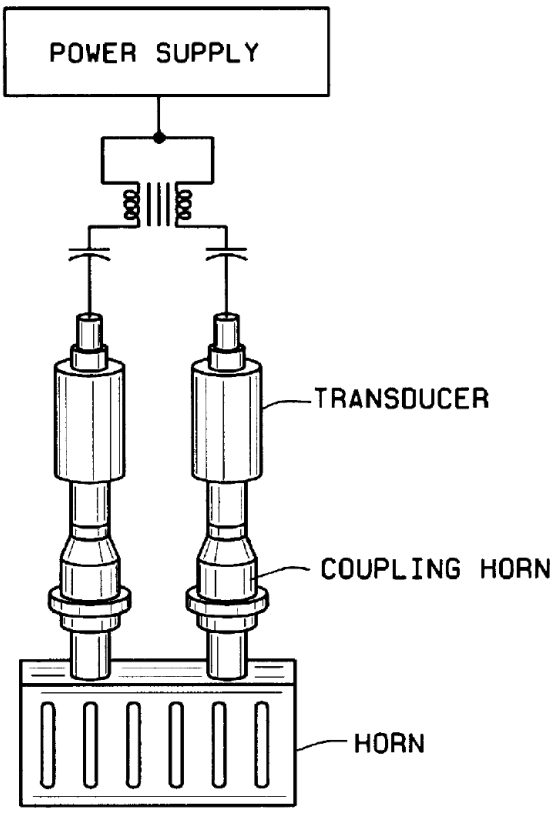

Figure 39 Balun schematic [14]

The stack included two 1:1.5 gain boosters and a single Branson Ultrasonics rectangular slotted riser back 1:3 gain horn made of uncoated titanium. It was 152.4 mm long with a 12.7 mm wide front face and a 38.1 mm back stock. The system was set to the energy mode, meaning that the power supply monitored dissipated power

as a function of time and discontinued the weld cycle once a preselected value of energy had been delivered to the part [6]. The FFS machine in this study was equipped with servo motor end seal control.

All rolls of film material were fed into the FFS machine such that the metallized OPP layer of the film was on the inside of the bag, at the faying surfaces. The machine was set to manual mode and a chain of five empty bags was created for each treatment. The blade that separates the bags was removed from the machine for safety reasons so the chain of bags was separated by a paper cutter with a sliding metal blade. Each bag specimen was labeled and material ID, cycle number, specimen number, production rate, energy, amplitude, peak power, peak energy, and ultrasonic on time were documented.

Peel strength was determined by following the ASTM International D882-12 Standard test method for tensile properties of thin plastic sheeting [9]. Elongation aspects of ASTM D882 were not used. Specimens were cut to the proper size and shape requirements outlined in ASTM D882.

One 25 mm wide strip was cut from the left side of the vertical seal of each bag using a paper cutter with sliding metal blade as shown in Figure 40. The strip was subsequently cut in half crosswise with ceramic scissors and labeled so the top and bottom welds could both be analyzed. Specimen length varied from 65 to 150 mm, and specimens of excessive length were trimmed using ceramic scissors.

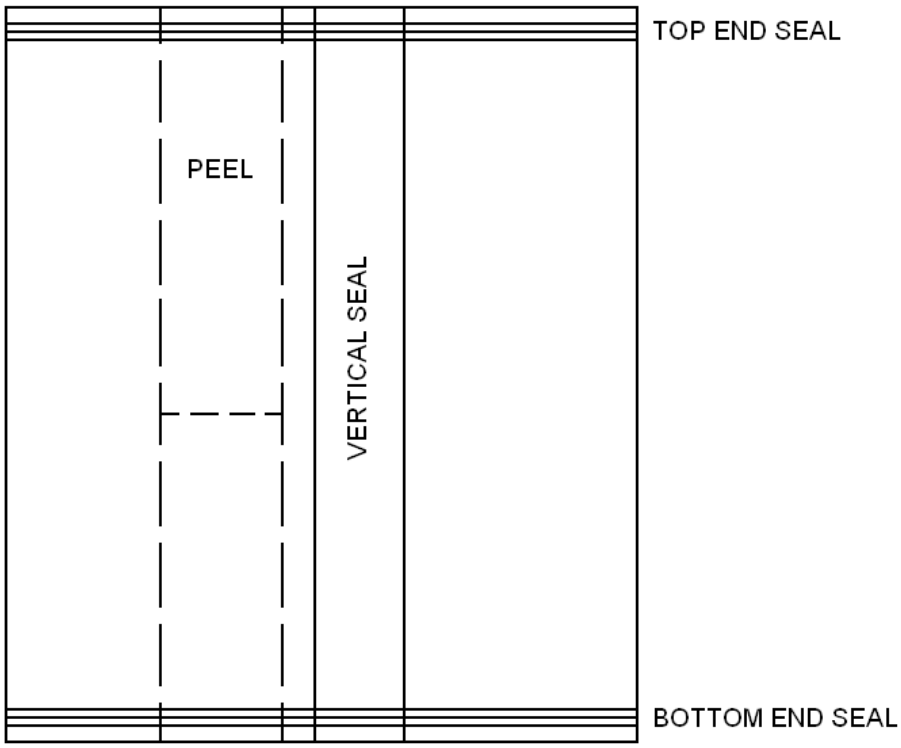

Figure 40 Schematic of peel test specimen location from bag specimen

Peel strength measurements were completed with an Instron (Norwood, MA) Model 4502 load frame with grip distance of 50 mm and crosshead speed of 25 mm/min. Mechanical wedge action grips were used, and the grip surface itself was covered with 0.5 mm thick Nexcare Absolute Waterproof First Aid Tape to prevent slip and puncture of the specimens due to the sharp diamond serrated finish on the face of the jaw grips.

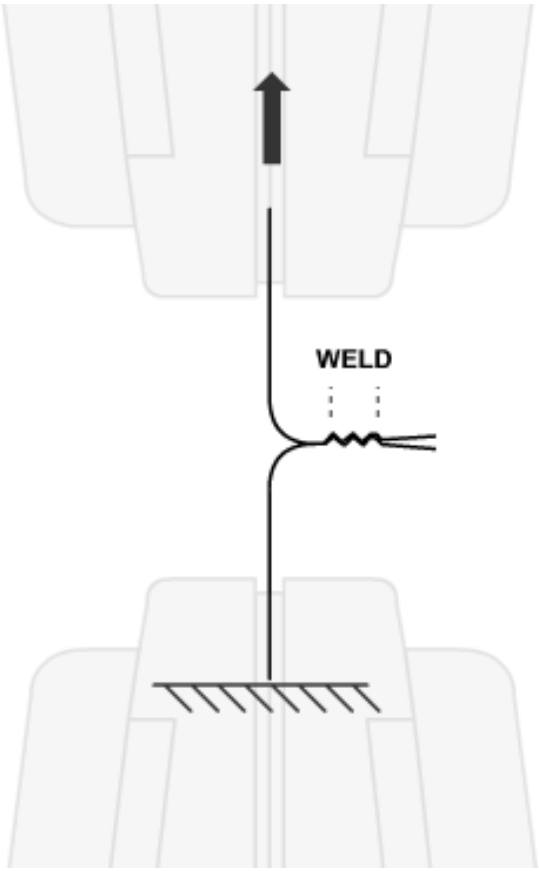

Figure 41 Diagram of specimen placement for peel strength testing

Both legs of the sample were placed into the grips such that the weld was centered between the grips as shown in Figure 41. The bottom grip remained stationary, and the top grip traveled 20 mm upward or until the weld failed. The measured maximum load was documented.

Results and Discussion

There were three objectives of the experiments in the work, namely to determine 1) proper production rate, 2) proper amplitude, and 3) proper energy to produce relatively strong welds. While it was anticipated that weld strength (peel strength) would be generally inversely proportional to weld energy and amplitude,

it was also anticipated that welds made with excessively low weld energy and amplitude would be weak as a result of under welding. Results ranged from 1.2 to 14 N for peel strength of top welds and 1.7 to 17 N for bottom welds.

The response variable, peel strength, was plotted as function of energy for the top and bottom welds of each of the six materials. Spline curve lines were added in all of the graphs and are shown for visualization only. While they approximate the response as a continuous curve across energy levels, response data only exists at discrete energy values. All error bars correspond to one standard deviation with a population of five samples.

These results were then analyzed in JMP statistical software using 3-way Analysis of Variance (ANOVA) with replications to identify statistically significant relationships between the three single term and four cross term explanatory variables and the three response variables (see Table 10). Effects tests tables were created to determine the probability values, or p-values, for each explanatory variable. Low p-values, below the 0.05 level of significance adjusted for the total number of effects as shown in Equation (6), indicate that the means of the response variables were dependent on the explanatory variables.

Table 10 Seven main and interaction effects for FFS welds

Main Effects	**Interaction Effects**
Energy	Energy and Amplitude
Amplitude	Energy and Production Rate
Production Rate	Amplitude and Production Rate
	Energy, Amplitude, and Production Rate

$$\alpha = \frac{0.05}{7} = 0.007 \qquad (6)$$

Finally, all results were analyzed in JMP to determine if statistically significant relationships existed between the three single term and four cross term explanatory variables and the coefficient of variance, $C_v = \frac{\sigma}{\mu}$, for peel strength. That is to say, statistical tests were conducted to determine whether the independent variable affected the repeatability of the dependent variables. However, none of the tests were found to be statistically significant and those results are not detailed.

Top Weld Results

Table 11does not show significant effects for materials F2A or PW. The mean peel strength for materials F2B, PW, and YH were not differentiable for all of the welding parameters, and there was no relationship between peel strength and welding parameters, as shown in Figure 42 and Figure 46.

The p-values for peel strength in Table 11 show evidence of a significant effect of production rate on peel strength for the F2B, F8, and YH materials. In Figure 43 and Figure 44, it is seen that the lower production rate, 80 bpm, consistently resulted in higher weld strength, regardless of energy or amplitude, for the top weld of materials F2B and F8, respectively. It is believed that slow production rates resulted in less vibration of the frame of the system and allowed the system to maintain proper alignment during the welding cycle. It is also seen that there is no general trend for peel strength as a function of amplitude or energy, other than at the slow rate and lower amplitude. It is believed that the lower

amplitude resulted in long weld cycles, again allowing the system to stabilize, resulting in less machine frame vibrations.

Although it is counterintuitive, peel strength of the top weld was generally proportional to production rate for the YH material. as shown in Figure 47. It is believed that this observation is an anomaly resulting from experimental error. Table 11 also indicates an interaction effect between energy and amplitude for the YH material. The relationship is seen in Figure 47 by the inversely proportional relationship between peel strength and energy for the lower amplitudes and the proportional relationship at the 0.032 mm amplitude. This suggests that this film required less energy to weld and that the high amplitude promoted the onset of burn through and over welding.

As seen from Table 11, for material CB there was a statistically significant effect on peel strength as a function of energy, which is also seen in Figure 45. Here, peel strength is generally proportional to energy. This may have been the result of higher energies promoting better fusion and therefore higher weld strength; however, there was no evidence of reaching a critical energy value beyond which over welding was seen.

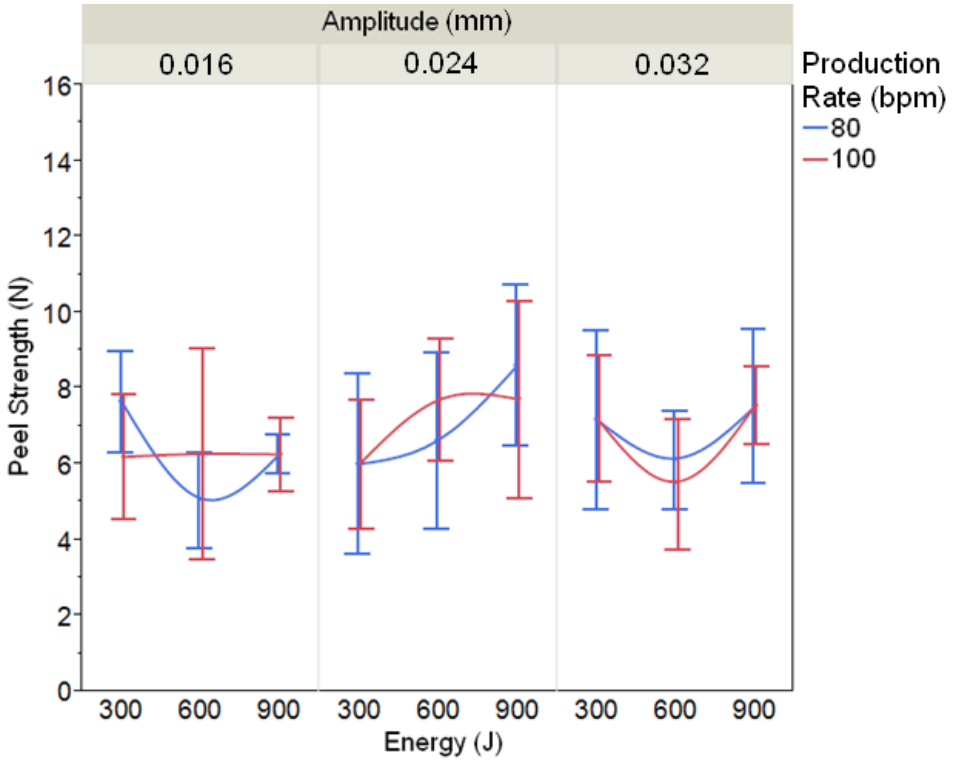

Figure 42 Peel strength (N) as a function of energy (J) for top weld of F2A

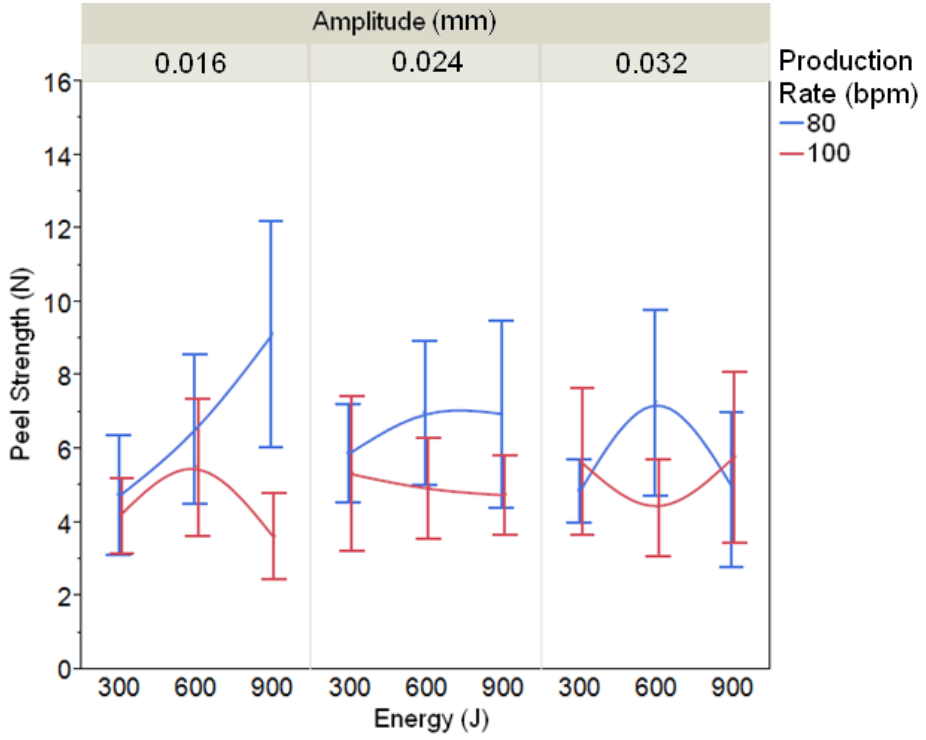

Figure 43 Peel strength (N) as a function of energy (J) for top weld of F2B

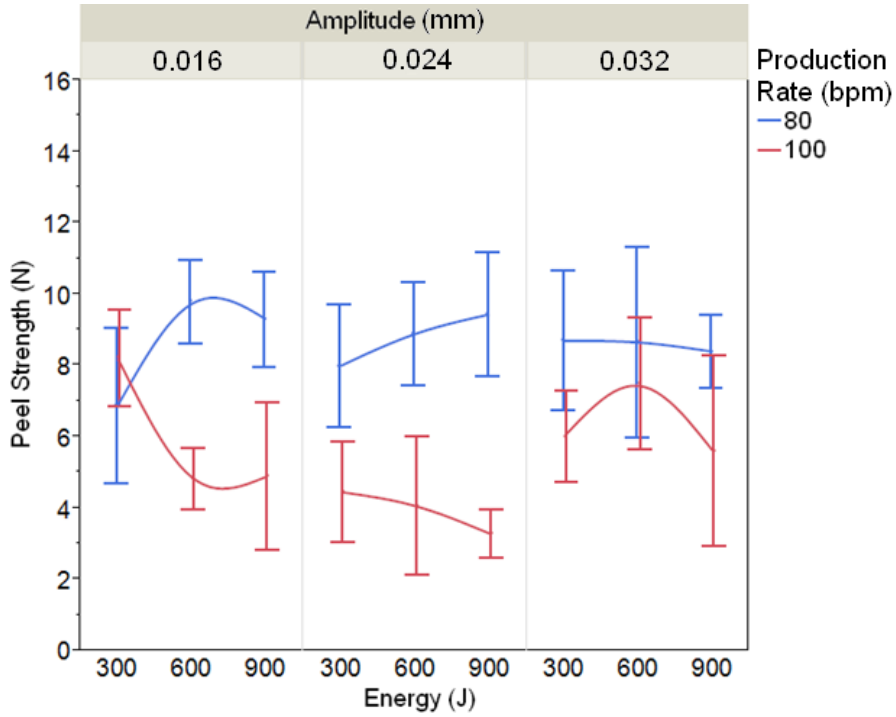

Figure 44 Peel strength (N) as a function of energy (J) for top weld of F8

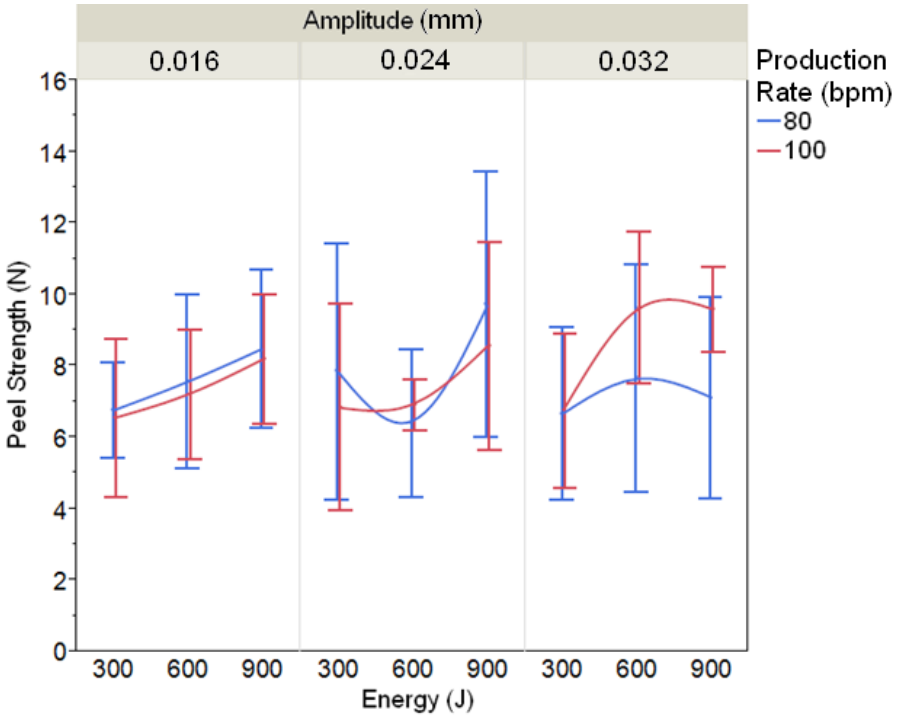

Figure 45 Peel strength (N) as a function of energy (J) for top weld of CB

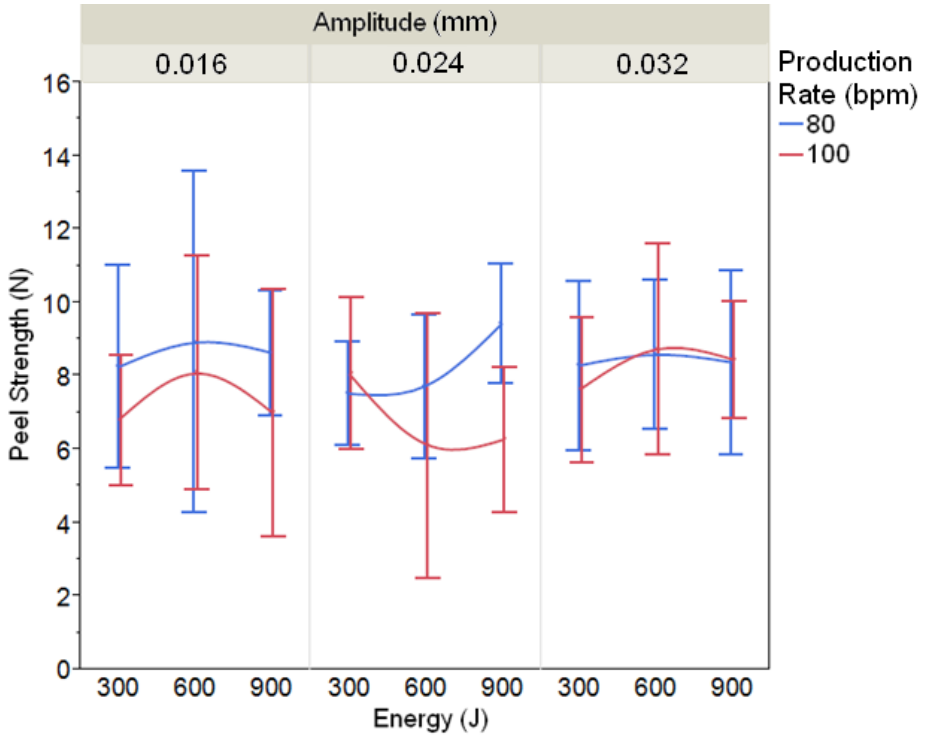

Figure 46 Peel strength (N) as a function of energy (J) for top weld of PW

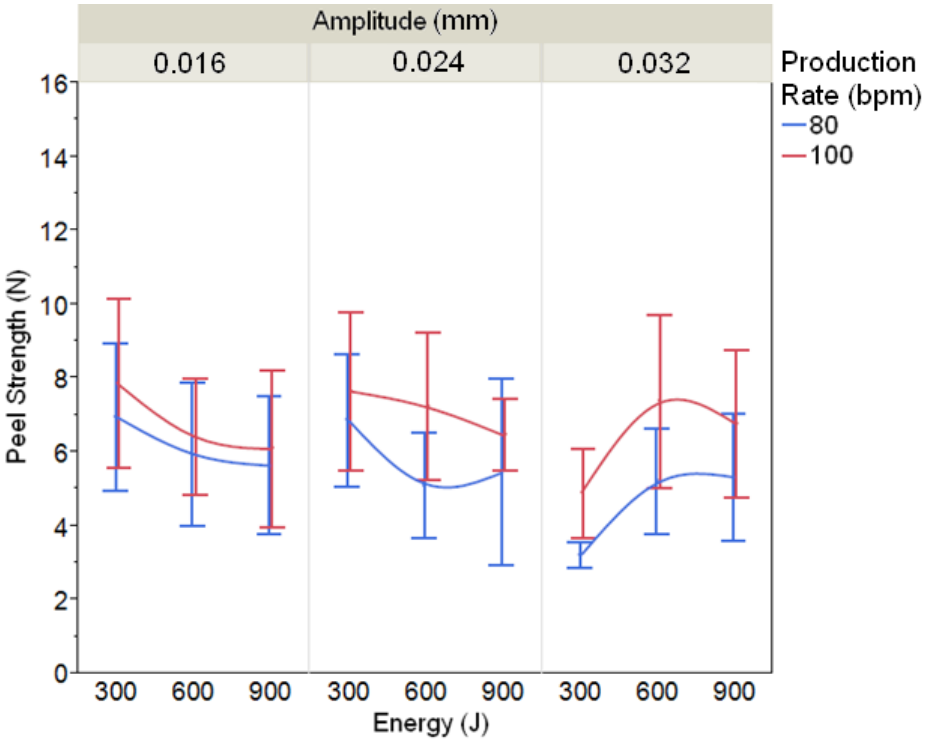

Figure 47 Peel strength (N) as a function of energy (J) for top weld of YH

Table 11 P-values for peel strength for top weld

Source of Variation	Material ID					
	F2A	F2B	F8	CB	PW	YH
Production Rate	0.9665	0.0005*	<0.0001*	0.6601	0.0732	0.0041*
Energy	0.1881	0.1351	0.7612	0.0070*	0.6781	0.3659
Production Rate×Energy	0.7976	0.0295	0.0082	0.5610	0.4131	0.9842
Amplitude	0.3295	0.7708	0.6645	0.4776	0.5441	0.0426
Production Rate×Amplitude	0.8482	0.0482	0.5357	0.1483	0.3704	0.2498
Energy×Amplitude	0.5062	0.1294	0.9379	0.9789	0.9190	0.0044*
Production Rate×Energy ×Amplitude	0.4875	0.0405	0.0316	0.4141	0.7700	0.8268

*p-value < α, indicates significant difference in means

Bottom Weld Results

P-values for all effects for the bottom weld of all materials are shown in Table 12. Only three of the materials showed a significant difference in peel strength for any of the independent variables: those materials were F2A, F8, and CB.

While there is no clear explanation as to why the bottom weld was less affected by welding parameters, it is suggested that this phenomenon was related to the weld configuration. More specifically, the top weld was subjected to a pulling action during the welding process as the material was folded and transported between the welding head. The force helped promote burn through as the molten film was "ripped" apart when excessive energy was applied. This pulling force was not seen (in our case where no food was in the bag) in the lower seal, making the process more robust and less affected by the welding parameters.

As indicated in Table 12 and seen in Figure 48 and Figure 50, peel strength is generally inversely proportional to production rate for materials F2A and F8. The lower production rate, 80 bpm, consistently resulted in higher peel strength for these materials. Again, this was most likely the result of vibration within the machine frame.

Similar to the results for the top weld, Table 12 showed a significant effect on peel strength as a function of energy for the bottom weld of the CB material. This is also seen in Figure 51, where peel strength is generally proportional to energy. This may have been the result of higher energy promoting better fusion and therefore higher weld strength.

Table 12 shows no significant effects for materials F2B, PW, or YH. The mean peel strength for these materials were not differentiable for all of the welding parameters, and there was no relationship between peel strength and welding parameters, as shown in Figure 49, Figure 52, and Figure 53.

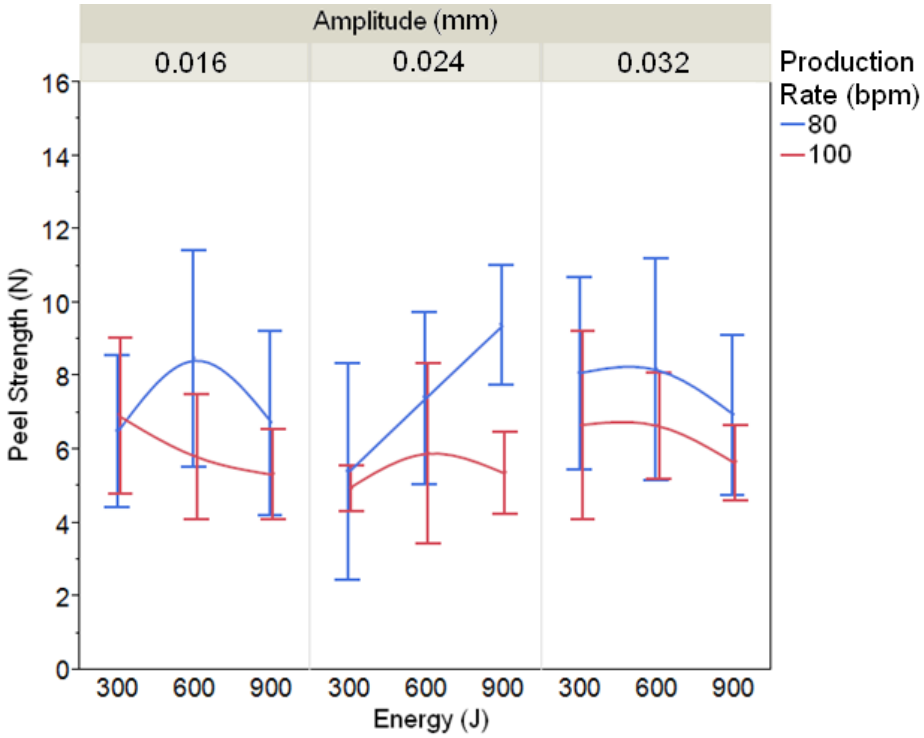

Figure 48 Peel strength (N) as a function of energy (J) for bottom weld of F2A

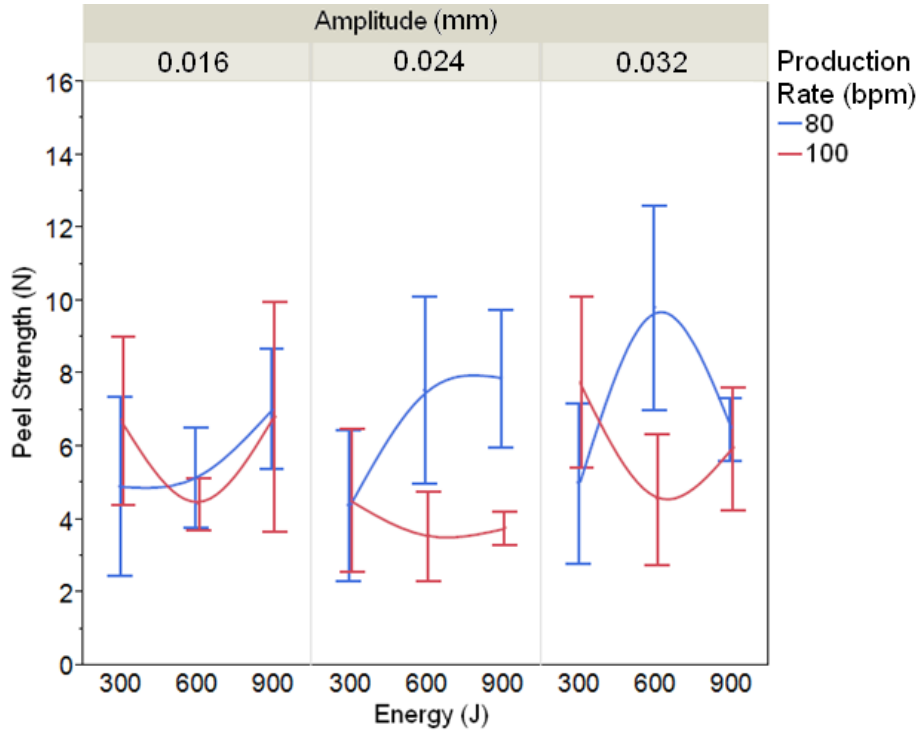

Figure 49 Peel strength (N) as a function of energy (J) for bottom weld of F2B

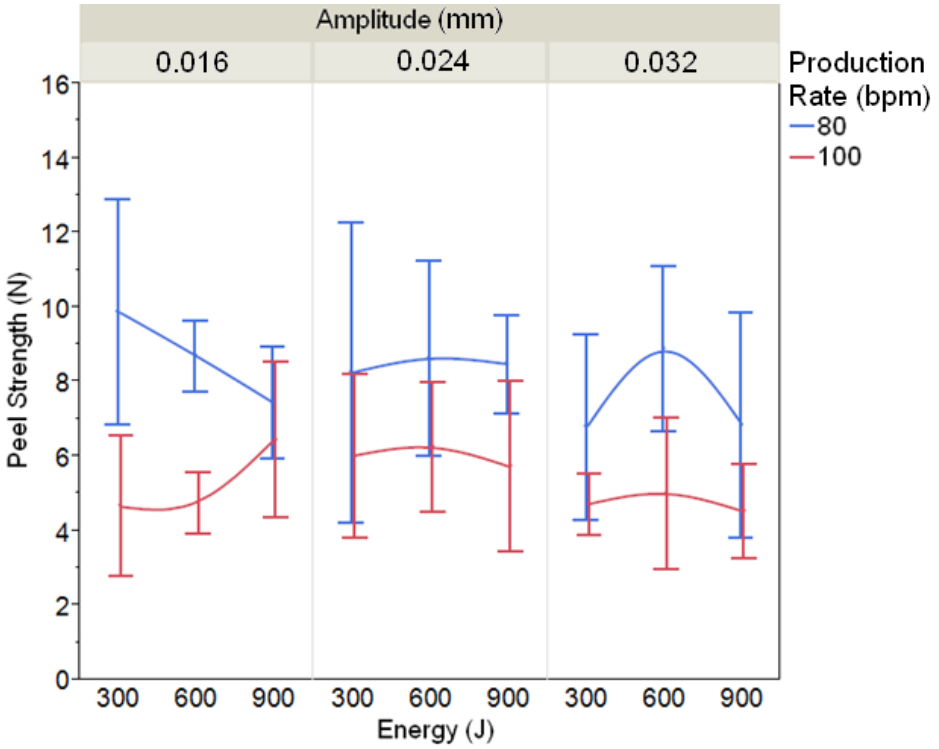

Figure 50 Peel strength (N) as a function of energy (J) for bottom weld of F8

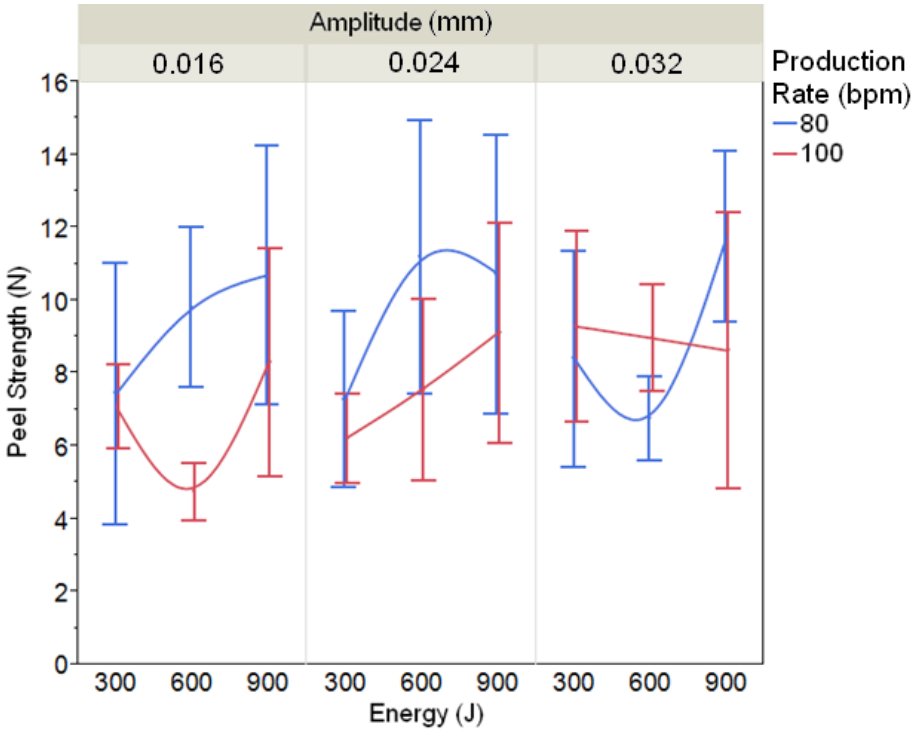

Figure 51 Peel strength (N) as a function of energy (J) for bottom weld of CB

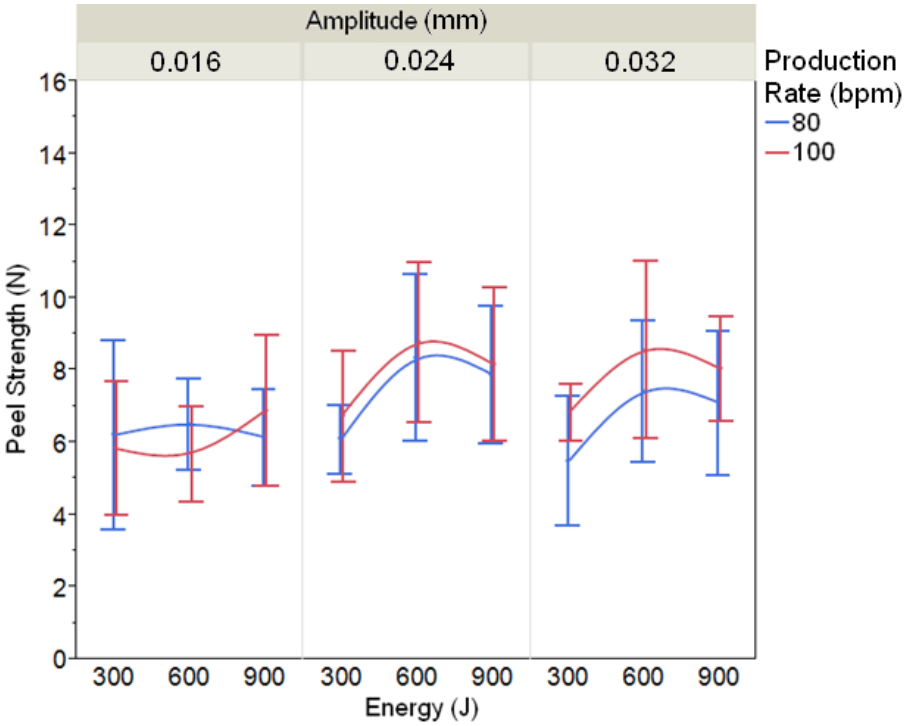

Figure 52 Peel strength (N) as a function of energy (J) for bottom weld of PW

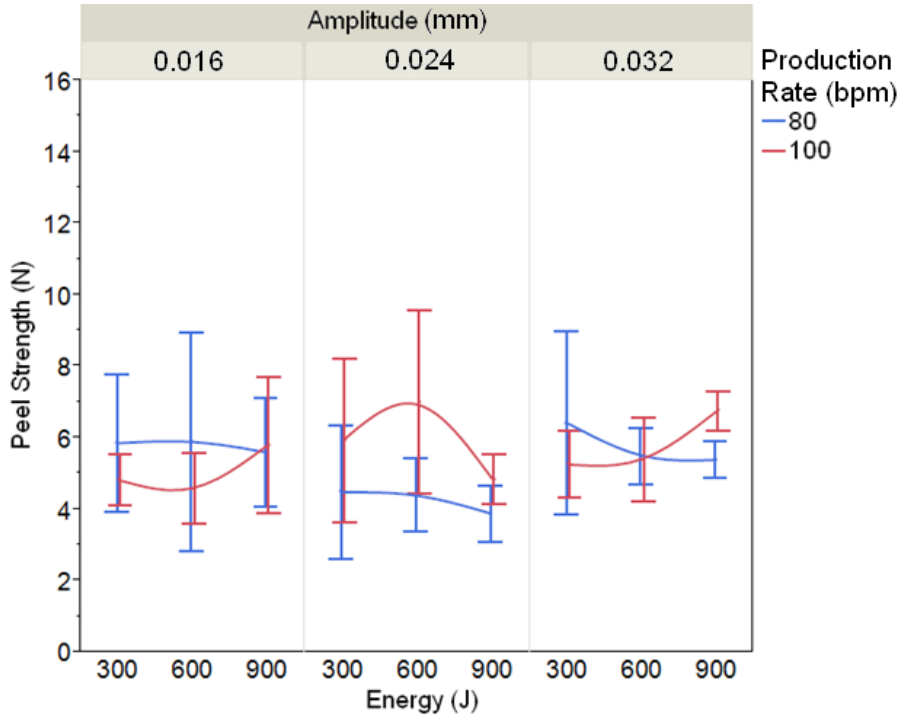

Figure 53 Peel strength (N) as a function of energy (J) for bottom weld of YH

Table 12 P-values for peel strength for bottom weld

Source of Variation	Material ID					
	F2A	F2B	F8	CB	PW	YH
Production Rate	0.0011*	0.0288	<0.0001*	0.0140	0.2252	0.3280
Energy	0.8400	0.1917	0.7807	0.0048*	0.0182	0.8856
Production Rate×Energy	0.1264	0.0088	0.3179	0.1980	0.8965	0.3423
Amplitude	0.4832	0.2076	0.1284	0.1677	0.0375	0.4332
Production Rate×Amplitude	0.8653	0.2885	0.6067	0.0685	0.1866	0.3641
Energy×Amplitude	0.7972	0.3821	0.8227	0.6105	0.4414	0.8434
Production Rate×Energy ×Amplitude	0.4875	0.6672	0.1151	0.5672	0.5355	0.5587

*p-value < α, indicates significant difference in means

Conclusions

The aim of this study was to identify the set of parameters that yielded the highest peel weld strengths for ultrasonic end seal welds of coextruded polyolefin bags created on a FFS machine. Three explanatory variables—energy, amplitude, and production rate—were investigated to determine whether any of them had a significant effect on peel strength, shear strength, or tearing force. It was expected that excessive welding resulting from excessive energy and/or amplitude may result in lower weld strengths.

Materials CB and YH both exhibited unexplained effects in both end seals. Low energy levels resulted in low peel strength for both the top and bottom weld for the CB material. The slower production rate for the top weld of the YH material also correlated with lower peel strength. Furthermore, there was a significant interaction effect for the top weld of YH. The effect of energy on peel strength

changed for different amplitude levels. The lowest energy resulted in the highest peel strength for lower amplitude levels but in the lowest peel strength at high amplitudes. Not enough is known about either material to make definitive explanations for these peculiarities; however, neither of these materials was modified to lower coefficient of friction. It is possible that some of the slip modifier in the other materials may have migrated to the weld interface during welding, enhancing these effects.

Neither lower energy nor amplitude resulted in significantly stronger welds. The only significant effect that behaved as predicted was the production rate for materials F2B and F8 for the top weld and materials F2A and F8 for the bottom weld. In both cases, lower production rate resulted in higher peel strength.

The lower production rate, 80 bpm, is slightly slower than what is understood to be the industry standard, but it results in stronger welds for three of the materials. However, no weld peel strength standard has been provided so it is possible that even the lower strength welds are sufficient so long as they are reasonably airtight.

CHAPTER 4. GENERAL CONCLUSIONS

General Discussion

The studies in both Chapters 2 and 3 involved ultrasonic welding of six coextruded polyolefin films. The goal of these studies was to identify the set of parameters that yielded the highest weld strengths and least amount of experimental error. Energy, amplitude, and weld force were varied on a bench top plunge welding system in the first study. In the second, energy, amplitude, and production rate parameters were varied in a vertical form fill seal machine used to create bags. It was expected that excessive welding resulting from excessive energy and/or force and/or amplitude could result in lower weld strengths.

Welds made on the bench top system were evaluated using three measures of weld strength: peel strength, shear strength, and tearing force. Only the shear strength results behaved as predicted. Here, lower energy and weld force had a significant relationship with higher strength for all materials. Results for peel and tearing force, while including some significant effects, were not conclusive. Results were analyzed to determine whether a single set of parameters resulted in high peel strength, shear strength, and tear resistance simultaneously. It was seen that the 0.032 mm amplitude and 620 N weld force resulted in relatively high peel and shear strength as well as tear resistance for the majority of the materials. There was no single energy level that resulted in relatively high weld strengths for all responses. The 400 J level resulted in the highest peel strength welds for all materials, the 300 J

setting had high shear strength outputs for half of the materials, and the highest tear resistance was recorded most often at the 200 J level. In general the optimized weld parameters for all three response variables, would be at amplitude of 0.032 mm, weld force of 620 N, and weld energy of 300 J.

The second study evaluated the peel strength of top and bottom end seals of bags created on a high volume packaging machine. For the top weld, the highest peel strength did correlate with low energy and amplitude levels for material YH. The lower production rate also resulted in higher weld strength for the top weld of materials F2B and F8 and the bottom weld of materials F2A and F8.

In addition, all the results were analyzed to determine whether statistically significant relationships existed between the independent variables and the coefficient of variance for each of the response variables. The tests were not found to be statistically significant for peel strength or tear resistance; however, energy, weld force, and an interaction effect between energy, weld force, and amplitude were found to be significant sources of variation in shear strength in the first study for several of the materials. It is believed that some combinations of these parameters resulted in excessive heating. In this instance, over weld occurred and welds were weak. If this did not occur, strong welds were created consistently.

Although some clear trends were identified, results for the two studies are inconclusive because of inconsistent results. For example, in Chapter 2, high weld force resulted in high peel strength and very low shear strength for all materials and high tearing force for the "F" materials. This makes it difficult to determine an optimal weld force for overall strength defined by these three measurements. In Chapter 3, results were inconsistent between the top and bottom weld. These welds are made simultaneously with the same equipment and settings. A set of optimal parameters that would work for both top and bottom seal was not determined.

Recommendations for Future Research

The anonymous material provider originally wanted welds to be created and studied in all three possible joint configurations, variable OPP to variable OPP, variable OPP to metallized OPP, and metallized OPP to metallized OPP. Only the metallized OPP to metallized OPP arrangement has been studied thus far. The first recommendation is to conduct studies using the other two possible configurations.

A second recommendation is to more thoroughly examine the differences in the variable layer of the six materials to determine how they impacted the results of these studies. For example, the three "F" materials oftentimes had similar results and the other three materials reacted much differently. However, it is known that some of the materials were modified to decrease the coefficient of friction. During welding it was also casually observed that some materials were noisier. Some fed through the FFS machine with more tension than others, causing bunching around

the forming shoulder and wrinkles at the end seals. Some films even caused the polyurethane film advance belts to shed small bits of material. Not enough is known about the materials at the time of publication to make an informed inference to explain any of these differences.

Finally, in the packaging industry cost, production volumes, and meeting customer requirements are key metrics. Maximizing weld strength may not be the highest priority for customers, such as convenience food manufacturers. However, on-the-shelf aesthetics are becoming increasingly important. The parameters that result in the best looking, most reliable, and fastest welds that meet the minimum strength criteria are more than likely going to be the ones chosen. A final recommendation for further research would be to investigate the influence of weld parameters on those other key performance criteria: aesthetics, reliability, and speed.

APPENDIX A. BENCH TOP WELDING PARAMETERS

Weld Mode	Energy
Pretrigger	Off
Max Timeout	2.000 s
External U/S Delay	Off
Cycle Aborts	Off
Ground Detect Abort	Off
Control Limits	Off
Collapse Cutoff	Off
Absolute Cutoff	1.0000 in
Peak Power Cutoff	Off
Hold Time	Off
Afterburst	Off
Afterburst Delay	0.100 s
Afterburst Time	0.100 s
Afterburst Amplitude	100%
Energy Braking	Off
Post Weld Seek	Off
Frequency Offset	Off
Digital Tune	30001
Test Amplitude	100%
Actuator Clear Output	Off
Distance	0.1250 in
Missing Part	Off
Missing Part Abort Min	Off
Missing Part Abort Max	Off

Limits

Reject Limits	Off
Reject Reset Required	Off
+ R Collapse Limit	Off
- R Collapse Limit	Off
+ R Energy Limit	Off
- R Energy Limit	Off
+ R Absolute Limit	0.9500 in
- R Absolute Limit	0.9000 in
+ R Power Limit	Off
- R Power Limit	Off
+ R Time Limit	Off
- R Time Limit	Off
+ R Weld Force Limit	Off
- R Weld Force Limit	Off
+ R Trigger Distance Limit	Off

- R Trigger Distance Limit	Off
+ R Band Limit	Off
- R Band Limit	Off
+ R Freq Limit	30229 Hz
- R Freq Limit	29537 Hz
Suspect Limits	Off
Suspect Reset Required	Off
+ S Collapse Limit	Off
- S Collapse Limit	0.0140 in
+ S Energy Limit	Off
- S Energy Limit	Off
+ S Absolute Limit	Off
- S Absolute Limit	Off
+ S Power Limit	Off
- S Power Limit	Off
+ S Time Limit	Off
- S Time Limit	Off
+ S Weld Force Limit	Off
- S Weld Force Limit	Off
+ S Trigger Distance Limit	Off
- S Trigger Distance Limit	Off

Visual Quality Limits

Weld Time Min	Off
Energy Min	Off
Peak Power Min	Off
Weld Collapse Min	0.0140 in
Total Collapse Min	Off
Total Absolute Min	Off
Weld Force Min	Off
Total Cycle Time Min	Off
Weld Time Max	Off
Energy Max	Off
Peak Power Max	Off
Weld Collapse Max	0.0180 in
Total Collapse Max	Off
Total Absolute Max	Off
Weld Force Max	Off
Total Cycle Time Max	Off

Aed/aod Settings

Velocity	
Column Position	
Horn	~3:1 gain
Booster	Gold, 1:1.5 gain
Downspeed Setting	1”/s
Fixture	

Digital UPS

Ramp Time	0.010 s
Memory	On
Weld Status	On
Preset Name	Defaut
Seek Time	0.500 s
Timed Seek	Off

System Information

Calibration	Factory
Power Supply	1500 W
Control Level	F
Frequency	30 kHz
SW Version	10.30
SBC SW Version	10.30
Calibration Date Run	11/28/12
Actuator	aed/aod
Cylinder Diameter	2.00 in
Cylinder Stroke	4.00 in
PS Lifetime Counter	9637
Preset Count	25
Overloads	510
General Alarm	2895
PS Serial Number	xmh07032776
Act Serial Number	06115490D
Power Supply	Digital

System Configuration

Language	English
Units	USCS
Password	Off
Start Screen	Main
RS232	Host
Baud Rate	9600
General Alarm Reset Required	Off
Trigger Beeper	On
Error Beeper	On
Alarm Beeper	On
Amplitude Control	Internal
Extra Cooling	Off
Weld Scale	1X
Test Scale	1X
Digital Filter	On
Ext Presets	Off
Decimal Place	2
Sequencing Presets	Off
J3-32 Input	Select Preset1
J3-33 Input	Select Preset2
J3-19 Input	Select Preset4
J3-17 Input	Select Preset8
J3-31 Input	Display Lock
J3-1 Input	Ext Signal
J3-36 Output	Disabled
J3-8 Output	Disabled
J3-22 Output	Disabled
User Inputs	0V
Ext Start Dly	5.000 s
Upper Limit	0V
Ground Detect	0V
Welder Addr	Off
Frequency Offset	Internal
Hand Held	Off
Distance	Start Switch

Printer

Printing	On
Weld Data on Sample	Off
Power Graph on Sample	Off
Amplitude Graph on Sample	Off
Frequency Graph on Sample	Off
Col Distance Graph on Sample	Off
Velocity Graph on Sample	Off
Force Graph on Sample	Off
Weld History on Sample	Off
Setup on Sample	Off
Weld Data on Alarm	Off
Power Graph on Alarm	Off
Amplitude Graph on Alarm	Off
Frequency Graph on Alarm	Off
Col Distance Graph on Alarm	Off
Velocity Graph on Alarm	Off
Force Graph on Alarm	Off
Weld History on Alarm	Off
Setup on Alarm	Off
X Axis Scale	0.500 s
Welds per Page	50

APPENDIX B. FFS MACHINE PARAMETERS

End Seal Control

	Approach	Seal	Retract
Distance	1.9950 inches	1.0000 inches	0.2500 inches
Velocity	12 in/s	3 in/s	12 in/s
Acceleration	500 in/s^2	500 in/s^2	500 in/s^2
Deceleration	500 in/s^2	500 in/s^2	500 in/s^2
Force Target	100.0%		
Force Feedback	0%		

Machine Timing 1

	Start	End
Film Advance	0°	200°
Vertical Seal Start	185°	
Vertical Seal Dwell	0.500 s (300 machine degrees)	
Vertical Seal Cool	On	
Vertical Cool	0°	
End Seal	130°	355°
Ultrasonic Start	175°	
Ultrasonic Dwell	1.000 s (600 machine degrees)	
Ultrasonic Cool	Off	
Ultrasonic Cool	140°	230°

Sealing Control

Vertical Seal	Temp Actual	384°F
	Temp Setpoint	°F
Ultrasonic	Amplitude	100%
	Energy	1000 J
	Peak % Power	0 %
	Current % Power	0 %
	Peak Energy	0 J
	Current Energy	0 J
	Actual On Time	0.000 s
	Force Feedback	0 %
	Start Run	On
	Seek	On
	Tune	On
	Fault	

APPENDIX C. INSTRON PARAMETERS

Test Control

Direction	Up
Channel	Position
Crosshead Speed	25 mm/min
Speed Change	None
Peak 1 Level	0%
Load Cell	10 kN

Test Limit

Break Detect	1 kN

Absolute Limit

High Load	9 kN
High Extension	508 mm

Limit Control

Set method limit on console	
Data Sampling Rate	10 points/second

Screen Calculations

MAX.STR	Max Stress (MPa)
MAX.LOAD	Maximum Load (kN)
%STN.MAX	Maximum Strain (%)
TOUGHNESS	Toughness (MPa)
XDISP.MAX	Maximum Displacement (mm)
ENERGY1	Energy (J)
ENERGY.BRK	Energy at Break (J)

Printer Calculations

Stress at Max.Load	Max Stress (MPa)
Modulus (Aut Young)	Young's Modulus (MPa)
Max % Strain	Maximum Strain (%)
Stress at User Break	Stress at User Defined Break (MPa)

REFERENCES

[1] "Global sustainable packaging market to double to $170B by 2014," 2010.

[2] Sustainable Packaging Coalition, "Definition of sustainable packaging," August 2011. [Online]. Available: http://sustainablepackaging.org. [Accessed 19 March 2013].

[3] R. Coles, D. McDowell and M. J. Kirwan, Eds., Food packaging technology, Oxford: Blackwell, 2003.

[4] Branson Ultrasonics Corporation. “Ultrasonic welders,” [Online]. Available: http://www.emersonindustrial.com. [Accessed 8 March 2013].

[5] D. A. Grewell and A. Benatar, "Welding of plastics: Fundamentals and new developments," *International polymer processing,* vol. 22, no. 1, pp. 43-60, 2007.

[6] D. A. Grewell, A. Benatar and J. B. Park, Eds., Plastics and composites welding handbook, Munich: Hanser, 2003.

[7] Modern plastics and C. A. Harper, Eds., Modern plastics handbook, New York: McGraw-Hill, 2000.

[8] American Welding Society, *Specification for standardized ultrasonic welding test specimen for thermoplastics,* 1999.

[9] ASTM International, *Standard test method for tensile properties of thin plastic sheeting,* 2012.

[10] W. F. Riley, L. D. Sturges and D. H. Morris, Statics and mechanics of materials: An integrated approach, 1st ed., New York: Wiley, John & Sons, 1995.

[11] ASTM International, *Standard test method for propagation tear resistance of plastic film and thin sheeting by pendulum method,* 2009.

[12] Y. V. Kissin, "Elmendorf tear test of polyethylene films: Mechanical interpretation and model," *Macromolecular materials and engineering,* vol. 2011, no. 296, pp. 729-743, 2011.

[13] A. Agresti and B. Finlay, Statistical methods for the social sciences, 4th ed., Upper Saddle River, NJ: Prentice Hall, 2009.

[14] A. J. Roberts, "Ultrasonic apparatus". United States Patent 5,828,156, 23 October 1996.

ACKNOWLEDGEMENTS

My family, Don, Diane, Kevin, and Emily have always supported and encouraged all of my endeavors and this one has been no different. Thanks go to them for their advice, interest, and help with machining and sample preparation.

I would like to thank my committee chair, especially Dr. David Grewell, and my committee members, Drs. Raj Raman and Michael Kessler, for their time and support of this project. Other faculty, Drs. Robert Stephenson and Steven Freeman, and staff, Kris Bell, Peggy Best, and Jess Higgins were also very helpful.

I am grateful to the Center for Industrial Research and Service staff for their support and encouragement throughout my entire graduate college experience, especially Steven Devlin.

Special thanks go to Hans Neisser and Sophie Morneau and everyone at Branson Ultrasonics Corporation who made this project possible. Thanks also to M. and his company for use of their films. Others who volunteered time and talent on this project certainly did not go unappreciated: Liz, Andrew, Matt, Mom, Jamile, Andy, Mike, and Nick. Thanks also to all my friends, especially Sara, Rachel, Alan and Nate, who provided advice and interest, but most of all just listened.

Lastly, I have not forgotten those who provided even the smallest amount of education, materials, and machine time on previous research attempts: Dad, Drs. Robert Anex, Carl Bern, Doug Stokke, and Ken Moore. Also: Russ Hoffman, Sargent Metal Fabricating, Uncle Jim, Roger Hintz, and Mark Hanna. Thank you.